R. & M. No. 3008
(18,148)
A.R.C. Technical Report

MINISTRY OF SUPPLY

AERONAUTICAL RESEARCH COUNCIL
REPORTS AND MEMORANDA

Velocity Distribution on Thin Tapered Arrowhead and Delta Wings with Spanwise Constant Thickness Ratio at Zero Incidence

By

S. NEUMARK, Techn.Sc.D., F.R.Ae.S., J. COLLINGBOURNE, B.Sc.,
and E. J. YORK, B.Sc.

LONDON : HER MAJESTY'S STATIONERY OFFICE
1958
THIRTEEN SHILLINGS NET

Velocity Distribution on Thin Tapered Arrowhead and Delta Wings with Spanwise Constant Thickness Ratio at Zero Incidence

By

S. Neumark, Techn.Sc.D.,† J. Collingbourne, B.Sc.†

and E. J. York, B.Sc.‡

Communicated by the Principal Director of Scientific Research (Air)
Ministry of Supply

Reports and Memoranda No. 3008*

May, 1955

Summary.—This report is a continuation of four earlier ones by the present authors and contains a theoretical investigation of subsonic flow past thin tapered swept-back wings at zero incidence, by the first-order method. The basic theory is followed by the results of computation carried out on the Automatic Computing Engine of the National Physical Laboratory, for several groups of plan-forms, partly of arrowhead and partly delta type, with varying sweepback, aspect ratio and taper, the profile being biconvex parabolic and thickness ratio constant spanwise. The results are illustrated by graphs of isobar patterns on 36 wings.

1. *Introduction.*—This report is the fifth of the series by the present authors dealing with the calculation of velocity distribution and critical Mach numbers for thin wings with symmetrical profiles, of various plan-forms, at zero incidence. In three previous reports[1, 2, 3], untapered swept-back wings of infinite and finite aspect ratio were considered, and a procedure for determining critical Mach numbers was worked out. The first-order (linear perturbation) method, based on continuous systems of sources and sinks, was used, and explicit solutions were obtained not only in the simplest case of biconvex parabolic profile but also for some alternative profiles. In a subsequent paper[4] unswept tapered (rhombus) wings with spanwise constant thickness ratio were considered, and it was found that, even with parabolic profile, the results would not be reduced to explicit formulae in terms of elementary or tabulated functions. Numerical results could be obtained only by laborious expansions into infinite series and complicated desk computation. This method seemed inadequate to deal with the most complex problem of swept-back tapered-wing plan-forms (including delta wings), and it was suggested that automatic computers should be used in this case. By permission of the Director, National Physical Laboratory, such computation has been carried out on the Automatic Computing Engine (A.C.E.) for a suitably chosen group of wing plan-forms, and the results are presented here.

* R.A.E. Report Aero. 2545, received 16th January, 1956.
† Of the Royal Aircraft Establishment.
‡ Of the National Physical Laboratory.

The wings considered in this paper, as in Ref. 4, have a constant thickness ratio spanwise, and both profile chord and thickness decrease in proportion, linearly from root to tips. Two groups of wings have been dealt with, the first one consisting of a number of arrowhead plan-forms (with leading and trailing edges both swept-back, *cf.* Fig. 3), the second one of delta plan-forms (with trailing edges unswept, *cf.* Fig. 4).

A preliminary small computation on the A.C.E. has been made for a group of unswept tapered (rhombus) wings, and the results, presented in Table 1 and illustrated in Fig. 5, agreed very satisfactorily with those obtained previously in Ref. 4. It was then decided to proceed with the larger computational programme, and the results are given in Tables 2 and 3, and illustrated by graphs of isobar patterns on 36 arrowhead and delta wings, of small and large taper ratio (Figs. 8 to 11). In each of four groups, there are 9 wings, mutually affine according to Göthert's rule, so as to provide a basis for determining critical Mach numbers.

Alternative cases of thickness ratio varying spanwise are of equal importance, and one interesting case is that of thickness ratio decreasing linearly spanwise, *i.e.*, the profile thickness decreasing parabolically from root to tips. This case, which happens to lead to explicit though highly complicated solutions in terms of elementary functions, was treated briefly by Fiul[5] and investigated in more detail by Newby in a report[6] being issued simultaneously with the present one; a comparison of results should be of particular interest.

An acknowledgment is due to the Director of the N.P.L. and the Staff of its Mathematics Division for the magnificently efficient work on the A.C.E., which provided in a matter of days results that would otherwise have required years; also to Dr. S. H. Hollingdale for his advice and help in this matter. The complicated graphs have been prepared by Miss F. M. Ward.

2. *Fundamental Formulae.*—The general theory has been developed in previous papers[1, 2, 3] and in particular, for tapered wings, in Ref. 4. It has been found that the supervelocity v_{xr} at any point P on the surface of a swept-back tapered wing with biconvex parabolic profile (Fig. 1), contributed by the right-hand half of the sources and sinks system, is given by:

$$\frac{\pi v_{xr}}{U\vartheta} = \int_0^s \left\{ \frac{1}{r_1} + \frac{1}{r_2} + \frac{1}{b(1-\bar{y}/s')} \ln \frac{r_2 - (b - x - \bar{y}\tan\varphi_L)}{r_1 + (b + x + \bar{y}\tan\varphi_T)} \right\} d\bar{y} \,. \qquad (2.1)$$

This is the same formula as (I.2) in Ref. 4, except that the upper limit of integration is now s instead of s', to allow for cropping. The integrand represents the contribution of an infinitesimal strip QQ′ of source and sink elements at the distance $\bar{y}$ from the symmetry plane, of width $d\bar{y}$. The co-ordinates of P are x and y, and r_1, r_2 represent the distances PQ, PQ′ from P to the strip ends, expressed by:

$$\left.\begin{aligned} r_1^2 &= (b + x + \bar{y}\tan\varphi_T)^2 + (\bar{y} - y)^2 \\ r_2^2 &= (b - x - \bar{y}\tan\varphi_L)^2 + (\bar{y} - y)^2 \end{aligned}\right\} \,. \qquad (2.2)$$

The formula (2.1) will be made dimensionless by introducing the usual symbols:

$$\left.\begin{aligned} \varepsilon &= b/s', \qquad \psi = c_t/c_r = 1 - s/s' \\ \eta' &= y/s', \qquad \bar{\eta} = \bar{y}/s', \qquad \xi = \frac{x + y\tan\varphi_0}{b - \varepsilon y} \end{aligned}\right\} , \qquad (2.3)$$

where ε is coefficient of convergence, ψ taper ratio, and η', $\bar{\eta}$, ξ dimensionless co-ordinates chosen in such a way that η' and $\bar{\eta}$ vary spanwise from 0 to $(1 - \psi)$ when moving from root to tip, and ξ varies chordwise from (-1) to $(+1)$ when moving from trailing to leading edge. Observing that:

$$\tan\varphi_0 = \tan\varphi_L - \varepsilon = \tan\varphi_T + \varepsilon \,, \qquad (2.4)$$

we obtain from (2.3):

$$\left.\begin{aligned} b + x &= s'\{\varepsilon(1-\eta')(1+\xi) - \eta' \tan\varphi_T\} \\ b - x &= s'\{\varepsilon(1-\eta')(1-\xi) + \eta' \tan\varphi_L\} \end{aligned}\right\}, \quad .. \quad .. \quad .. \quad .. \quad .. \quad .. \quad (2.5)$$

and the formula (2.1) becomes:

$$\frac{\pi v_{xr}}{U\vartheta} = \int_0^{1-\psi} \left\{ \frac{1}{\rho_1} + \frac{1}{\rho_2} + \frac{1}{\varepsilon(1-\bar\eta)} \ln \frac{\rho_2 + (\bar\eta - \eta')\tan\varphi_L - \varepsilon(1-\eta')(1-\xi)}{\rho_1 + (\bar\eta - \eta')\tan\varphi_T + \varepsilon(1-\eta')(1+\xi)} \right\} d\bar\eta \quad (2.6)$$

where:

$$\left.\begin{aligned} \rho_1^2 &= \{\varepsilon(1-\eta')(1+\xi) + (\bar\eta - \eta')\tan\varphi_T\}^2 + (\bar\eta - \eta')^2 \\ \rho_2^2 &= \{\varepsilon(1-\eta')(1-\xi) - (\bar\eta - \eta')\tan\varphi_L\}^2 + (\bar\eta - \eta')^2 \end{aligned}\right\}. \quad .. \quad .. \quad .. \quad (2.7)$$

The third term of the integrand in (2.6) becomes infinite for $\bar\eta = \eta'$, so that the integral is improper. This integral can be transformed in the following way. We integrate by parts and simplify the indefinite integral:

$$\int \ln \frac{\rho_2 + (\bar\eta - \eta')\tan\varphi_L - \varepsilon(1-\eta')(1-\xi)}{\rho_1 + (\bar\eta - \eta')\tan\varphi_T + \varepsilon(1-\eta')(1+\xi)} \frac{d\bar\eta}{1-\bar\eta} =$$

$$= -\ln(1-\bar\eta) \ln \left| \frac{\rho_2 + (\bar\eta - \eta')\tan\varphi_L - \varepsilon(1-\eta')(1-\xi)}{\rho_1 + (\bar\eta - \eta')\tan\varphi_T + \varepsilon(1-\eta')(1+\xi)} \right|$$

$$+ \varepsilon(1-\eta') \int \left(\frac{1+\xi}{\rho_1} + \frac{1-\xi}{\rho_2} \right) \frac{\ln(1-\bar\eta)}{\bar\eta - \eta'} d\bar\eta \,. \quad .. \quad .. \quad .. \quad .. \quad (2.8)$$

Introducing the limits of integration in the first term, and substituting (2.8) into (2.6), we obtain:

$$-\frac{\pi v_{xr}}{U\vartheta} = \frac{1}{\varepsilon} \ln\psi \ln G + I_1 + I_2 \,, \quad .. \quad .. \quad .. \quad .. \quad .. \quad .. \quad .. \quad (2.9)$$

where

$$G = \frac{\sigma_2 + (1 - \psi - \eta')\tan\varphi_L - \varepsilon(1-\eta')(1-\xi)}{\sigma_1 + (1 - \psi - \eta')\tan\varphi_T + \varepsilon(1-\eta')(1+\xi)}, \quad .. \quad .. \quad .. \quad .. \quad (2.10)$$

$$\left.\begin{aligned} I_1 &= -\int_0^{1-\psi} \left\{ 1 + (1-\eta')(1+\xi) \frac{\ln(1-\bar\eta)}{\bar\eta - \eta'} \right\} \frac{d\bar\eta}{\rho_1} \\ I_2 &= -\int_0^{1-\psi} \left\{ 1 + (1-\eta')(1-\xi) \frac{\ln(1-\bar\eta)}{\bar\eta - \eta'} \right\} \frac{d\bar\eta}{\rho_2} \end{aligned}\right\}, \quad .. \quad .. \quad .. \quad .. \quad (2.11)$$

and σ_1, σ_2 are the values of ρ_1, ρ_2 for the upper limit of integration $(1 - \psi)$:

$$\left.\begin{aligned} \sigma_1^2 &= \{\varepsilon(1-\eta')(1+\xi) + (1 - \psi - \eta')\tan\varphi_T\}^2 + (1 - \psi - \eta')^2 \\ \sigma_2^2 &= \{\varepsilon(1-\eta')(1-\xi) - (1 - \psi - \eta')\tan\varphi_L\}^2 + (1 - \psi - \eta')^2 \end{aligned}\right\}. \quad .. \quad .. \quad (2.12)$$

The present formulae clearly exhibit the singularity at $\bar\eta = \eta'$. This singularity makes the integrals I_1, I_2 unsuitable for automatic integration, but this difficulty may be overcome by extracting the singularity in the simplest form, and writing:

$$\left.\begin{aligned} I_1 = -\int_0^{1-\psi} \Bigg\{ 1 &+ \frac{(1-\eta')(1+\xi)}{\bar\eta - \eta'} \ln \frac{1-\bar\eta}{1-\eta'} \\ &- \frac{\ln(1-\eta')}{\varepsilon} \frac{\rho_1 - \varepsilon(1-\eta')(1+\xi)}{\bar\eta - \eta'} \Bigg\} \frac{d\bar\eta}{\rho_1} - \frac{\ln(1-\eta')}{\varepsilon} \int_0^{1-\psi} \frac{d\bar\eta}{\bar\eta - \eta'} \\ I_2 = -\int_0^{1-\psi} \Bigg\{ 1 &+ \frac{(1-\eta')(1-\xi)}{\bar\eta - \eta'} \ln \frac{1-\bar\eta}{1-\eta'} \\ &- \frac{\ln(1-\eta')}{\varepsilon} \frac{\rho_2 - \varepsilon(1-\eta')(1-\xi)}{\bar\eta - \eta'} \Bigg\} \frac{d\bar\eta}{\rho_2} - \frac{\ln(1-\eta')}{\varepsilon} \int_0^{1-\psi} \frac{d\bar\eta}{\bar\eta - \eta'} \end{aligned}\right\}. \quad (2.13)$$

In (2.13), the first integrals of I_1 and I_2 are easily seen to be proper, while only the two last simple ones are improper, but these may be found in the elementary way. Substituting (2.13) into (2.9), we obtain the final formula for v_{xr}:

$$-\frac{\pi v_{xr}}{U\vartheta} = \frac{1}{\varepsilon}\ln\psi\ln G + \frac{2}{\varepsilon}\ln(1-\eta')\ln\frac{\eta'}{1-\eta'-\psi} + I_A + I_B, \qquad \ldots\ldots \quad (2.14)$$

where I_A, I_B denote the following proper integrals:

$$\left.\begin{aligned} I_A = &-\int_0^{1-\psi}\left\{1+\frac{(1-\eta')(1+\xi)}{\bar\eta-\eta'}\ln\frac{1-\bar\eta}{1-\eta'}\right. \\ &\left.-\frac{\ln(1-\eta')}{\varepsilon}\frac{2\varepsilon(1-\eta')(1+\xi)\tan\varphi_T+(\bar\eta-\eta')\sec^2\varphi_T}{\rho_1+\varepsilon(1-\eta')(1+\xi)}\right\}\frac{d\bar\eta}{\rho_1} \\ I_B = &-\int_0^{1-\psi}\left\{1+\frac{(1-\eta')(1-\xi)}{\bar\eta-\eta'}\ln\frac{1-\bar\eta}{1-\eta'}\right. \\ &\left.+\frac{\ln(1-\eta')}{\varepsilon}\frac{2\varepsilon(1-\eta')(1-\xi)\tan\varphi_L-(\bar\eta-\eta')\sec^2\varphi_L}{\rho_2+\varepsilon(1-\eta')(1-\xi)}\right\}\frac{d\bar\eta}{\rho_2} \end{aligned}\right\}, \qquad \ldots\ldots \quad (2.15)$$

and G, ρ_1, ρ_2, σ_1, σ_2 are given in (2.10), (2.7) and (2.12).

The supervelocity v_{xl} contributed by the left-hand half of the sources and sinks system might be determined in a similar way, but a much simpler procedure can be adopted. This contribution is exactly the same as that produced by the right-hand half of the system at the point P_1 (Fig. 1) situated in the left-hand part of the wing symmetrically to P. The only change in the previous formulae thus consists in changing the sign of y which means that, in (2.3):

η' must be replaced by $(-\eta')$,

and ξ must be replaced by $\xi_l = \dfrac{x - y\tan\varphi_0}{b+\varepsilon y} = \xi\dfrac{1-\eta'}{1+\eta'} - \dfrac{2\eta'}{1+\eta'}\dfrac{\tan\varphi_0}{\varepsilon}$,

the latter formula being written conveniently in two alternative forms, involving either the angle φ_T or φ_L:

$$\left.\begin{aligned} \varepsilon(1-\xi_l) &= \frac{\varepsilon(1-\eta')(1+\xi)}{1+\eta'} - \frac{2\eta'}{1+\eta'}\tan\varphi_T \\ \text{or} \qquad \varepsilon(1-\xi_l) &= \frac{\varepsilon(1-\eta')(1-\xi)}{1+\eta'} + \frac{2\eta'}{1+\eta'}\tan\varphi_L \end{aligned}\right\} \ldots\ldots \quad (2.16)$$

Applying this transformation, we obtain at once the following formulae for calculating v_{xl}, corresponding to (2.9 to 2.12):

$$-\frac{\pi v_{xl}}{U\vartheta} = \frac{1}{\varepsilon}\ln\psi\ln H + I_3 + I_4, \qquad \ldots\ldots \quad (2.17)$$

where

$$H = \frac{\sigma_4 + (1-\psi-\eta')\tan\varphi_L - \varepsilon(1-\eta')(1-\xi)}{\sigma_3 + (1-\psi-\eta')\tan\varphi_T + \varepsilon(1-\eta')(1+\xi)}, \qquad \ldots\ldots \quad (2.18)$$

$$\left.\begin{aligned} I_3 &= -\int_0^{1-\psi}\left[1+\left\{(1-\eta')(1+\xi) - \frac{2\eta'}{\varepsilon}\tan\varphi_T\right\}\frac{\ln(1-\bar\eta)}{\bar\eta+\eta'}\right]\frac{d\bar\eta}{\rho_3} \\ I_4 &= -\int_0^{1-\psi}\left[1+\left\{(1-\eta')(1-\xi) + \frac{2\eta'}{\varepsilon}\tan\varphi_L\right\}\frac{\ln(1-\bar\eta)}{\bar\eta+\eta'}\right]\frac{d\bar\eta}{\rho_4} \end{aligned}\right\} \ldots\ldots \quad (2.19)$$

$$\left.\begin{aligned} \rho_3^2 &= \rho_1^2 + 4\bar\eta\eta', \qquad \rho_4^2 = \rho_2^2 + 4\bar\eta\eta', \\ \sigma_3^2 &= \sigma_1^2 + 4(1-\psi)\eta', \quad \sigma_4^2 = \sigma_2^2 + 4(1-\psi)\eta' \end{aligned}\right\} \ldots\ldots \quad (2.20)$$

Both integrals I_3, I_4 are proper, and there is no need for further transformation.

3. *Simplified Formulae for Particular Cases.*—The above general formulae are determinate in all spanwise sections, except one case of the tip section of a cropped wing (where $\eta' = 1 - \psi$), in which case the two first terms of the formula (2.14) for the contribution of the right-hand-half system become infinite. The combination of two terms is indeterminate but, if we let η' tend to $(1 - \psi)$, then passing to the limit, we obtain:

$$\left(-\frac{\pi v_{xr}}{U\vartheta}\right)_{\eta' \to 1-\psi} = \frac{2}{\varepsilon} \ln \psi \ln \frac{1-\psi}{2\varepsilon\psi\sqrt{(1-\xi^2)}} + I_A + I_B , \quad \ldots \quad (3.1)$$

where I_A, I_B are given by (2.15) as before, with $(1 - \psi)$ substituted for η'.

The contribution of the left-hand-half system in this case is still given by the formula (2.17) which does not become indeterminate for $\eta' = 1 - \psi$.

Apart from this, there are a number of particular cases in which the general formulae assume more or less simplified forms. The more important cases are listed below:

(*a*) For fully tapered wings $s = s'$, $\psi = 0$, $\ln \psi = \infty$, and the first terms in (2.9), (2.14), (2.17), seem to be infinite. However, in this case σ_1 and σ_2 in (2.12) become equal, and similarly σ_3 and σ_4 in (2.20):

$$\left.\begin{aligned} \sigma_1^2 = \sigma_2^2 &= (1-\eta')^2\{(\varepsilon\xi + \tan\varphi_0)^2 + 1\} \\ \sigma_3^2 = \sigma_4^2 &= \sigma_1^2 + 4\eta' \end{aligned}\right\} \quad \ldots \quad (3.2)$$

It is then seen that $G = H = 1$ and, letting ψ tend to 0, we find that the first terms in (2.9), (2.14), (2.17) all vanish. The remaining terms are as before, with $\psi = 0$. The supervelocity at the tip becomes logarithmically infinite, as discussed in detail in Ref. 4.

(*b*) For delta wings (cropped or fully tapered) the general formulae apply, the only modification being that:

$$\varphi_T = 0 , \qquad \tan\varphi_0 = \varepsilon , \qquad \tan\varphi_L = 2\varepsilon . \quad \ldots \quad (3.3)$$

(*c*) For straight wings (rhombus plan-forms, cropped or fully tapered) the general formulae apply, a considerable simplification being that:

$$\varphi_0 = 0 , \qquad \tan\varphi_L = \varepsilon , \qquad \tan\varphi_T = -\varepsilon . \quad \ldots \quad (3.4)$$

We then obtain the formulae identical with those given in Ref. 4. In this case the wing (with biconvex parabolic profile) assumes fore-and-aft symmetry. The mid-chord line $\xi = 0$ becomes a locus of sectional supervelocity maxima, and hence acquires a particular importance. For this mid-chord line all formulae simplify greatly, *viz.*:

$$\left.\begin{aligned} \rho_1^2 = \rho_2^2 &= \varepsilon^2(1-\bar\eta)^2 + (\bar\eta - \eta')^2 \\ \rho_3^2 = \rho_4^2 &= \varepsilon^2(1-\bar\eta)^2 + (\bar\eta + \eta')^2 \\ \sigma_1^2 = \sigma_2^2 &= \varepsilon^2\psi^2 + (1 - \psi - \eta')^2 \\ \sigma_3^2 = \sigma_4^2 &= \varepsilon^2\psi^2 + (1 - \psi + \eta')^2 \end{aligned}\right\} \quad \ldots \quad (3.5)$$

Hence:

$$I_1 = I_2 , \qquad I_3 = I_4 , \qquad G = \frac{\sigma_1 - \varepsilon\psi}{\sigma_1 + \varepsilon\psi} , \qquad H = \frac{\sigma_3 - \varepsilon\psi}{\sigma_3 + \varepsilon\psi} , \quad \ldots \quad (3.6)$$

and formulae (2.9), (2.19) become:

$$\left.\begin{aligned} -\frac{\pi v_{xr}}{2U\vartheta} &= \frac{1}{2\varepsilon}\ln\psi\ln G - \int_0^{1-\psi}\left\{1 + (1-\eta')\frac{\ln(1-\bar\eta)}{\bar\eta - \eta'}\right\}\frac{d\bar\eta}{\rho_1} \\ -\frac{\pi v_{xl}}{2U\vartheta} &= \frac{1}{2\varepsilon}\ln\psi\ln H - \int_0^{1-\psi}\left\{1 + (1+\eta')\frac{\ln(1-\bar\eta)}{\bar\eta + \eta'}\right\}\frac{d\bar\eta}{\rho_3} \end{aligned}\right\} \quad \ldots \quad (3.7)$$

thus identical with (4.7) of Ref. 4. The first of (3.7) has the singularity at $\bar{\eta} = \eta'$ and, for automatic integration, should be replaced by (2.14), where I_A and I_B now become equal:

$$I_A = I_B = -\int_0^{1-\psi} \left\{ 1 + \frac{1-\eta'}{\bar{\eta}-\eta'} \ln \frac{1-\bar{\eta}}{1-\eta'} + \frac{\ln(1-\eta')}{\varepsilon} \frac{2\varepsilon^2(1-\eta') - (\bar{\eta}-\eta')(1+\varepsilon^2)}{\rho_1 + \varepsilon(1-\eta')} \right\} \frac{d\bar{\eta}}{\rho_1} . \quad .. \quad .. \quad (3.8)$$

It may be mentioned that, in the general case ($\varphi_0 \neq 0$), the locus of sectional supervelocity maxima is curved and not known in advance. It can only be determined when the entire supervelocity field has been computed.

(*d*) For all swept-back tapered-wing plan-forms, the supervelocity in the central section is obtained from the general formulae by putting $\eta' = 0$, which results in considerable simplification. The two parts v_{xr} and v_{xl} become equal, we have:

$$\left.\begin{aligned}
\rho_1^2 = \rho_3^2 &= \{\varepsilon(1+\xi) + \bar{\eta} \tan \varphi_T\}^2 + \bar{\eta}^2 \\
\rho_2^2 = \rho_4^2 &= \{\varepsilon(1-\xi) - \bar{\eta} \tan \varphi_L\}^2 + \bar{\eta}^2 \\
\sigma_1^2 = \sigma_3^2 &= \{\varepsilon(1+\xi) + (1-\psi) \tan \varphi_T\}^2 + (1-\psi)^2 \\
\sigma_2^2 = \sigma_4^2 &= \{\varepsilon(1-\xi) - (1-\psi) \tan \varphi_L\}^2 + (1-\psi)^2 \\
I_1 = I_3 &= -\int_0^{1-\psi} \left\{ 1 + (1+\xi) \frac{\ln(1-\bar{\eta})}{\bar{\eta}} \right\} \frac{d\bar{\eta}}{\rho_1} \\
I_2 = I_4 &= -\int_0^{1-\psi} \left\{ 1 + (1-\xi) \frac{\ln(1-\bar{\eta})}{\bar{\eta}} \right\} \frac{d\bar{\eta}}{\rho_2} \\
G = H &= \frac{\sigma_2 + (1-\psi) \tan \varphi_L - \varepsilon(1-\xi)}{\sigma_1 + (1-\psi) \tan \varphi_T + \varepsilon(1+\xi)}
\end{aligned}\right\} , \quad .. \quad .. \quad .. \quad .. \quad (3.9)$$

and the total supervelocity is given by:

$$-\frac{\pi v_x}{U\vartheta} = \frac{1}{\varepsilon} \ln \psi \ln G + I_1 + I_2 , \quad .. \quad .. \quad .. \quad .. \quad .. \quad .. \quad .. \quad .. \quad (3.10)$$

where there are no singularities in the integrands of I_1, I_2, and so no further transformation is necessary.

If, in addition, $\psi = 0$ (fully tapered wing), then the first term in (3.10) again disappears, and we come back to the formula (I.6) of Ref. 4.

4. *Programme and Summary of Computational Work.*—Several integrals appearing in the fundamental formulae are not expressible in terms of elementary or tabulated functions. Similar but simpler formulae for the case of unswept tapered wings were evaluated in a limited range by series expansions and desk calculating machines, as reported in Ref. 4. However, this method becomes impracticable in the wider field covered by this paper, and some sort of automatic computation had to be used. Upon agreement by the Director of the National Physical Laboratory, it was decided to carry out the work on the Automatic Computing Engine of the N.P.L., and the programme was worked out by the present writers on the following lines.

Each cropped swept-back tapered (double trapezium) plan-form, including delta, can be defined by the values of three parameters, e.g., ε, ψ and φ_0 (Fig. 1). A number of combinations had to be chosen with the view of obtaining most useful and characteristic results with a minimum of computational work. The main idea adopted in choosing the parameters was to obtain several families, each containing a considerable number of mutually ' affine ' plan-forms. This means that, within a family, each plan-form can be transformed into the others by a proportional

change of lateral co-ordinates (y). In such a way, each smaller plan-form becomes an analogous (Göthert's) transformation of each larger plan-form of the same family at a suitable Mach number (*see* Ref. 3, section 4.2 and Fig. 29).

It will be seen at once that, in affine transformation, the taper ratio ψ is invariant, while $\tan \varphi_0$ and ε vary in proportion, so that their ratio

$$\tan \varphi_0 / \varepsilon = K \quad .. \quad .. \quad .. \quad .. \quad .. \quad .. \quad (4.1)$$

is another invariant. It is convenient, therefore, to adopt a set of parameters involving K and ψ, and ε was left as the third one*. The parameter K describes an important feature of wing plan-forms: it increases with sweepback at any given value of the coefficient of convergence ε, and assumes the following values for various shapes:

$K = 0$ for unswept (rhombus) wings

$0 < K < 1$ for lozenge wings (swept-back leading and swept-forward trailing edges)

$K = 1$ for delta wings

$K > 1$ for arrowhead wings (swept-back leading and trailing edges).

It was decided to choose only two values of K:

$$K = 2{\cdot}5 \text{ and } K = 1 ,$$

and so to have one large group of swept-back wings with relatively large sweep, and another group of delta wings. The latter group, with its range of ψ and ε, covers practically the entire field of deltas, but the former one (with the same range of ψ and ε) is far from exhaustive but seems to provide a representative illustration.

The values of ψ originally suggested were: 0 (full taper), 0·15, 0·30 and 0·45 but, for technical reasons explained by E. J. York in the Appendix, it was decided to omit 0 (which is unrealistic anyhow), and adopt four values easily expressed as binary fractions, *viz.*:

$$\psi = \tfrac{1}{16} = 0{\cdot}0625; \quad \tfrac{1}{8} = 0{\cdot}125; \quad \tfrac{5}{16} = 0{\cdot}3125; \quad \tfrac{7}{16} = 0{\cdot}4375 .$$

It was proposed originally to have six values of ε for each family but, as variation of ε caused little trouble for the A.C.E. it was decided to adopt nine values in arithmetical progression: $\varepsilon = 0{\cdot}2(0{\cdot}1)1{\cdot}0$. This series of values gives comparatively more low than high aspect-ratio wings in each family of affine plan-forms, but this is convenient for calculating critical Mach numbers.

The total number of combinations of K, ψ and ε is $2 \times 4 \times 9 = 72$, and thus seventy-two wing plan-forms, forming four families of strongly swept-back wings (Fig. 3) and four families of deltas (Fig. 4) have been covered by computation.

The values of the co-ordinates ξ were throughout: $\xi = -0{\cdot}8(0{\cdot}2) + 0{\cdot}8$, so that there were nine points, distributed symmetrically fore-and-aft, in each section parallel to the plane of symmetry, and this was enough to draw a smooth curve according to the previous experience. As to the second co-ordinate η', it was originally planned to vary it through an interval of 0·1 (occasionally 0·05) but, for reasons explained in the Appendix, it was agreed to adopt the values easily expressed as binary fractions:

$$\eta' = 0; \quad \tfrac{1}{8} = 0{\cdot}125; \quad \tfrac{1}{4} = 0{\cdot}250; \quad \tfrac{3}{8} = 0{\cdot}375; \quad \tfrac{1}{2} = 0{\cdot}500; \quad \tfrac{9}{16} = 0{\cdot}5625;$$
$$\tfrac{5}{8} = 0{\cdot}625; \quad \tfrac{11}{16} = 0{\cdot}6875; \quad \tfrac{3}{4} = 0{\cdot}75; \quad \tfrac{7}{8} = 0{\cdot}875; \quad \tfrac{15}{16} = 0{\cdot}9375 ,$$

the largest value in each particular case being, of course, equal to $(1 - \psi)$ corresponding to the wing tip.

---

* The set of parameters adopted here does not include the aspect ratio. This, however, is simply connected with ε and ψ:

$$A = \frac{2}{\varepsilon} \frac{1 - \psi}{1 + \psi}, \quad .. \quad .. \quad .. \quad .. \quad .. \quad .. \quad (4{\cdot}2)$$

and does not depend on K. The values of A for various plan-forms are given in Figs. 3, 8, 9, 10 and 11.

Before the above large programme was started, a small preliminary computation had been performed for the particular case of supervelocity distribution along the mid-chord lines of (unswept) cropped rhombus wings, as considered in section 3, para. (*c*). This is the case partly covered by desk computation in Ref. 4, and the purpose was to have a reciprocal check of the two computing methods. The value of K was $K = 0$, and the values of ε, ψ and η' were exactly the same as in the large programme, *i.e.*, differing partly from those used in Ref. 4. The four families of the respective wing plan-forms are shown in Fig. 2. The results are given in Table 1, and the comparison with the previous ones gave an excellent agreement, whereupon it was decided to proceed with the larger scheme. The final results are contained in Tables 2 and 3 for swept-back and delta wings, respectively.

All computational results were received from the N.P.L. in the final form of printed copies prepared by the Electromatic Typewriter, and reproduced here directly as Tables 2 and 3, so that additional type-setting and thus any errors have been avoided.

5. *Analysis of Diagrams.*—Fig. 5 represents the supervelocity distribution along the mid-chord lines of two groups of cropped rhombus wings, with $\varepsilon = 0{\cdot}3$ and $0{\cdot}7$, respectively. The full lines have been obtained from Table 1 and hence represent the results of the preliminary computation on the A.C.E., while the broken lines illustrate the results of the desk computation (for $\psi = 0{\cdot}3$ and $0{\cdot}6$) given in Tables 4 and 5 of Ref. 4. It is seen that curves obtained in two different ways fit together very well, which is a reassuring check for both. Exactly similar agreement was obtained for several other values of ε (not illustrated here), and in view of this encouraging result it was decided to proceed with the remaining large scheme.

The results of the latter (as represented numerically in Tables 2 and 3) are somewhat too bulky to be illustrated fully. Complete graphs, representing chordwise distribution of v_x for all available values of the spanwise co-ordinate η' have been made for 36 plan-forms of Figs. 3 and 4 (those corresponding to the smallest and greatest values of taper ratio, $\psi = 1/16$ and $7/16$), but only two of these graphs, chosen as representative examples, are reproduced in this paper, Figs. 6 and 7; the former refers to a cropped arrowhead wing, the latter to a cropped delta, and the relevant form parameters are listed in the figures. Graphs like the two shown have been used for producing the isobar patterns, as in previous papers[1, 2, 3, 4]. Within the limitations of the linear theory, the isobars are identical with loci of constant v_x. Hence, intersecting the curves of $(-\pi v_x/4U\vartheta)$ of Figs. 6, 7, etc., by horizontal lines at prescribed ordinates (*e.g.*, $0{\cdot}2$, $0{\cdot}4$, $0{\cdot}6$, etc.), a sufficient number of points (ξ, η') of the respective isobars have been obtained for tracing them approximately on the wing plan-forms (Figs. 8, 9, 10 and 11). These figures present isobar patterns on 36 wings, the former two including groups of arrowhead wings, the latter two analogous groups of delta wings.

It should be noticed that the isobar parameter $(-\pi v_x/4U\vartheta)$ in Figs. 8 to 11 is the ratio of the local supervelocity to the maximum supervelocity in two-dimensional flow past the biconvex parabolic profile of the same thickness ratio as the given wing. The maximum value of the parameter in each case is a fraction smaller than 1, and this fraction shows the benefit of sweepback and taper in reducing the maximum incremental velocity in comparison with a straight untapered wing of large aspect ratio.

5.1. *Arrowhead Wings with a Very Small Taper Ratio* (Fig. 8, $\psi = 1/16$).—The first plan-form of this group has a very large aspect ratio and little sweepback and, as might be expected, the isobar pattern does not differ greatly from that on unswept (rhombus) plan-forms (*cf.* Ref. 4, Figs. 13 and 14). Most isobars intersect the root section at right angles and then tend to converge towards the (imaginary) sharp tip, being almost rectilinear through most of a semi-span. The maximum supervelocity, however, occurs not in the root section but at some two points (' foci ') located symmetrically on the two halves of the wing, and the ' highest ' isobars (*i.e.*, those with values of the parameter near the maximum) have the form of narrow closed ovals and do not reach the root section. It is clear that the small sweepback does not have much effect, and the effect of taper is almost as on unswept wings.

For subsequent plan-forms ε and φ_0 both increase gradually, and the isobar pattern changes considerably. The maximum supervelocity soon moves to the root section, and then all isobars cross this section at right angles. The shape of isobars in the kink region becomes rather similar to that occurring on swept untapered wings (*cf.* Ref. 1, 2, 3). Further outboard, the isobars are still forced to adjust their shape to that of the wing plan-form, so that the ' lowest ' ones are nearly convergent straight lines, except near the tips.

5.2. *Arrowhead Wings with a Large Taper Ratio* (Fig. 9, $\psi = 7/16$).—These wing plan-forms are obtained from the previous ones by cropping nearly half the semi-spans. Nevertheless, the isobar patterns do not differ very much from those in the preceding case, except that the tip effect is much more marked. The maximum supervelocities are located outboard originally but, as the sweep increases, they soon move to the root section.

The maximum supervelocity decreases again strongly as the wing contracts laterally. The actual values of these maxima do not differ much from those found in Fig. 8. It may be noticed, however, that in the cases of small sweepback, cropping reduces the maxima somewhat, while it increases them slightly on highly swept wings. This is a result similar to that found previously in Ref. 2.

The most important feature in both Figs. 8 and 9 is that the maximum supervelocities occur in the root sections on all wings with considerable sweepback and reduced aspect ratio (hence at high Mach numbers). The critical Mach numbers (at least ' lower criticals ') can therefore be calculated easily by considering only the conditions in the root section, on the lines of Ref. 3.

5.3. *Delta Wings with a Very Small Taper Ratio* (Fig. 10, $\psi = 1/16$).—The first few plan-forms of this group have large aspect ratio and little average sweep, and present isobar patterns even more similar to those on unswept (rhombus) wings, as given in Ref. 4, with maximum supervelocities outboard in both halves of the plan-form. There is also little difference from Fig. 8 but, as the average sweep is smaller, the maxima are somewhat higher. For subsequent, more and more contracted plan-forms, with ε and φ_0 increasing simultaneously, the isobar patterns behave quite differently from those in Fig. 8. The maxima do not move towards the root section but rather display a tendency to move further outboard towards the tips. The maxima decrease very slowly and, in the extreme cases of quite small aspect ratios, they are considerably higher than for corresponding arrowhead wings. This is clearly the effect of the sweepback being now consistently less than in the previous case.

5.4. *Delta Wings with a Large Taper Ratio* (Fig. 11, $\psi = 7/16$).—The result of cropping the wing plan-forms by nearly half the semi-spans again consists mainly in the tip effect. The maximum supervelocities are still located outboard in both halves of the wings but display no tendency to move towards the tips as the wing contracts. The maxima are reduced very slightly by cropping, and are still considerably higher than for analogous arrowhead wings.

For all delta wings, the calculation of (lower) critical Mach numbers will be somewhat more difficult than for arrowhead wings, because the maximum supervelocities do not occur in the root section but must be sought outboard, within the wing area. The respective points (' foci ') lie inside all the small oval isobars and cannot be determined with great accuracy, but this is not important. The values of the maxima may be determined with insignificant errors, and then the critical Mach numbers are easily determined, following the method of Ref. 3.

6. *Summing up, and Prospects of Further Progress.*—The present report brings to a conclusion most of the programme of theoretical research on velocity distribution over thin swept-back wings at zero incidence, by linear method, as originally proposed in 1947 (Ref. 1). Starting from the simple case of untapered wings with infinite aspect ratio and biconvex parabolic profile (where the only variable form parameter was the angle of sweep), it has been found possible to include gradually the effect of further geometrical features, such as finite aspect ratio[2], alternative profiles[3],

taper with no sweep[4], and finally the combination of sweepback, taper and aspect ratio as presented here. It must be noticed, however, that only spanwise constant thickness ratio and parabolic profile has been considered in the case of tapered plan-forms, but the alternative case of thickness ratio linearly decreasing spanwise is covered by Ref. 6. As the number of form parameters rises, the difficulties increase in a three-fold way:

(*a*) The fundamental theory becomes more and more complicated and, from a certain stage, the integrals involved are no longer reducible to explicit formulae in terms of tabulated functions

(*b*) The computation accordingly gets more and more formidable for each single wing until, in the case presented here, the only way to obtain numerical results is by the use of automatic computers

(*c*) Finally, with so many parameters, the field becomes so enormous that, to cover it adequately, even the automatic computation would require more time and money than available or even justifiable.

Similar difficulties are felt generally in aircraft design, since the progress in aerodynamics and propulsion has led to a bewildering variety of possible advantageous wing shapes which contrasts so strongly with the comparatively uniform plan-forms of the earlier period; and it must be realised that the present trend seems to complicate matters even more. The concepts of crescent and even more intricate plan-forms, with spanwise twist and variation of profile and thickness ratio lead to a position where neither theory nor experiment can treat more than particular cases, which give no real prospect of arriving at general conclusions.

From the above point of view, the results given in this paper must be regarded as of limited scope. Even so, thanks to the use of a powerful electronic computer, the illustration presented is really richer than could have been obtained by desk computation for previous simpler cases. The delta plan-forms (having 2 parameters only) are covered almost completely, with 36 combinations of taper and aspect ratios. The immense family of arrowhead wings is represented only by one (fairly typical) value of $K = 2{\cdot}5$, with similar combinations of taper and aspect ratios. It is easy, however, to predict at least qualitatively the effect of further increase of K, and nothing surprising would be expected from such a modification.

The wealth of information contained in the Tables 2 and 3 is such that it has not been possible yet to make full use of it. The present paper gives, in Figs. 8 to 11, a partial graphical illustration of the results, only for incompressible flow and four groups of wings, with the smallest and largest taper ratios, respectively. Four others (included in the Tables), with the intermediate values of taper ratio, have not been illustrated, especially as it has been found that they represent merely a gradual transition from one to the other extreme. The following further use of the data may be contemplated:

(i) In each of Figs. 8 to 11, the nine plan-forms are affine to each other with respect to x-axis, so that each smaller plan-form may be regarded as an analogous transformation, in Göthert's sense, of each larger one, at a certain Mach number. If, for example, the largest wing is taken as the true one (with some definite thickness ratio ϑ), then each of the remaining eight wings (contracted and thinned) may be used to obtain the velocity distributions and isobar patterns on the first one at eight consecutively increasing values of the Mach number M_0, with:

$$\frac{\tan\varphi}{\tan\varphi'} = \frac{\varepsilon}{\varepsilon'} = \frac{\vartheta'}{\vartheta} = \frac{A'}{A} = \sqrt{(1 - M_0^2)}; \quad v_{xc} = \frac{v_x'}{1 - M_0^2}, \qquad \ldots \qquad \ldots \quad (6.1)$$

where undashed symbols refer to the first wing, the dashed ones to respective contracted wings, v_x' is the supervelocity on any one of them in incompressible flow, and v_{xc} that on the first wing in compressible flow. A similar procedure will give the velocity distribution and isobar patterns on the second wing at seven consecutive Mach numbers corresponding to the following wings, and so on until, for the last wing but one, only one Mach number greater than 0 is available.

(ii) In the procedure described under (i), the maximum supervelocity on any chosen wing gradually increases with Mach number, and critical conditions are ultimately reached. Hence, a lower critical Mach number M_c may be calculated corresponding to any initial thickness ratio ϑ or, inversely, a ϑ corresponding to a chosen M_c (*cf.* Ref. 3). For arrowhead wings with a sufficiently large K (as in Figs. 8 and 9), only the conditions in the root section need be considered, but for delta wings the maxima must be looked for at appropriate places outboard. Isobar patterns need not be traced in either case, their value being merely illustrative.

(iii) The effect of change of profile on velocity distribution and critical Mach numbers may also be investigated, but this would require a vast amount of labour. If the profile has a sharp nose and thus is expressible by a polynomial in ξ (as profiles C and Q in Ref. 3), then the corrections to our formulae for the parabolic profile can be obtained in explicit (but not simple) form, thus avoiding further automatic computation. The profiles with rounded nose, however, would lead to formulae with highly complex transcedentals, and each wing would require an extremely involved automatic computation. Alternatively, Lighthill's method[7] might be used.

(iv) As regards the upper critical Mach numbers (*i.e.*, those at which sonic or supersonic conditions would spread over the entire surface), the position seems very difficult. The upper criticals have been defined in Ref. 3 only for untapered wings of large aspect ratio for which ' regular ' regions exist, with flow almost identical with that on infinite sheared wings. No such regions exist for tapered wings, and only in the case of arrowhead wings with large aspect ratio there may be regions with almost rectilinear converging isobars. Even in such cases, however, the definition of upper criticals will be doubtful, and the calculation will involve not only v_x, but also v_y components. As the conditions may be considerably affected by the transonic changes in the areas which have reached critical conditions earlier, the value of such a complicated investigation seems doubtful.

LIST OF SYMBOLS

A	Aspect ratio
A_n, B_n	Auxiliary expressions, *see* (A.5) and (A.6)
a_n	Auxiliary expression, *see* (A.13)
b	Semi-root chord
b_n	Auxiliary expression, *see* (A.14)
c_r	Root chord
c_t	Tip chord
d_n	Auxiliary expression, *see* (A.12)
F_1, F_2	Auxiliary functions, *see* (A.3) and (A.4)
f_n	Auxiliary expression, *see* (A.11)
G	Auxiliary function, *see* (2.10)
g_n	Auxiliary expression, *see* (A.10)

LIST OF SYMBOLS—*continued*

H	Auxiliary function, *see* (2.18)
I	(with appropriate suffices) integrals, *see* (2.11), (2.15) and (2.19)
K	Parameter, *see* (4.1)
$_n$	Suffix, assuming values 1, 2, 3, 4, *see* Appendix
r_1, r_2	Distances PQ, PQ′ in Fig. 1, *see* (2.2)
s	Wing semi-span
s'	Distance of point of intersection of wing leading and trailing edges from root chord
U	Undisturbed velocity of the airflow
v_x	x-component of the induced velocity (supervelocity)
v_{xr}, v_{xl}	Parts of v_x contributed by right-hand and left-hand parts of the sources and sinks systems, respectively
X_n	Auxiliary expression, *see* (A.9)
x, y	Chordwise and spanwise co-ordinates of a point on wing surface
$\bar{y}$	Spanwise co-ordinate of a source-and-sink strip QQ′ (Fig. 1), variable of integration, *see* (2.1)
Z_n	Auxiliary expression, *see* (A.7)
$\varepsilon = b/s'$	Coefficient of convergence, *see* Fig. 1
η'	Non-dimensional spanwise co-ordinate of a point on the right-hand part of the wing surface, *see* (2.3)
$\bar{\eta}$	Similar co-ordinate of a source-and-sink strip, *see* (2.3)
ϑ	Thickness ratio of wing profile, constant spanwise
ξ	Non-dimensional chordwise co-ordinate of a point on the right-hand part of the wing surface, *see* (2.3)
ξ_l	Similar co-ordinate on the left-hand part of the wing surface
ρ	(With appropriate suffices) auxiliary expressions, *see* (2.7) and (2.20)
σ	(With appropriate suffices) auxiliary expressions, *see* (2.12) and (2.20)
φ_0	Angle of sweepback of mid-chord line
φ_L, φ_T	Angles of sweepback of leading and trailing edge, respectively
φ_q	Angle of sweepback of quarter-chord line
ψ	Taper ratio, *see* (2.3)

REFERENCES

No.	Author	Title, etc.
1	S. Neumark ..	Velocity distribution on straight and swept-back wings of small thickness and infinite aspect ratio at zero incidence. R. & M. 2713. May, 1947.
2	S. Neumark and J. Collingbourne.	Velocity distribution on untapered sheared and swept-back wings of small thickness and finite aspect ratio at zero incidence. R. & M. 2717. March, 1949.
3	S. Neumark ..	Critical Mach numbers for thin untapered swept wings at zero incidence. R. & M. 2821. November, 1949.
4	S. Neumark and J. Collingbourne.	Velocity distribution on thin tapered wings with fore-and-aft symmetry and spanwise constant thickness ratio at zero incidence. R. & M. 2858. June, 1951.
5	A. Fiul	Finite wings at zero lift in subsonic flow. Northrop Aircraft Inc. Report R.A. 16. June, 1948.
6	K. W. Newby ..	The effects of taper on the supervelocities on three-dimensional wings at zero incidence. R. & M. 3032. June, 1955.
7	M. J. Lighthill ..	A new approach to thin aerofoil theory. *Aero. Quart.* Vol. III. November, 1951.

APPENDIX

Computation of Supervelocity on A.C.E.*

by E. J. York

1. It was required to compute $(-\pi v_x/4U\vartheta)$, where $v_x = v_{xr} + v_{xl}$, and the two components are given by the following formulae in the main text:

v_{xr} by (2.14), with auxiliary (2.7, 10, 12, 14)

v_{xl} by (2.17), with auxiliary (2.18, 19, 20).

The computation had to be done for three main groups of wing plan-forms, *viz.*, cropped rhombus (mid-chord line only), delta and highly swept-back tapered wings. Each plan-form was defined by three parameters ε, φ_0 and ψ or, making use of (4.1), by K, ε and ψ, where $K = 0$, 1 and 2·5 for rhombus, delta and swept-back wings, respectively. The angles of sweepback of the leading and trailing edges φ_L, φ_T, appearing in all formulae, are expressed, in virtue of (2.4) by:

$$\tan\varphi_L = (K+1)\varepsilon, \qquad \tan\varphi_T = (K-1)\varepsilon \qquad .. \quad .. \quad .. \quad .. \quad .. \quad \text{(A.1)}$$

2. The expressions are rewritten below, in a form which indicates the manner in which they were actually computed, and introduce extra symbols for certain of the quantities computed and stored by the A.C.E.

$$-\frac{\pi v_x}{4U\vartheta} = \tfrac{1}{4}\{F_1(\psi) - F_2(\psi)\}, \quad .. \quad .. \quad .. \quad .. \quad .. \quad .. \quad .. \quad .. \quad \text{(A.2)}$$

where

$$\left.\begin{aligned} F_1(\psi) &= \frac{1}{\varepsilon}\left[\ln\psi\ln\frac{A_2A_4}{A_1A_3} + 2\ln(1-\eta')\ln\frac{\eta'}{1-\psi-\eta'}\right], \quad \text{for } 1-\psi-\eta' \neq 0 \\ &\text{(if } \eta' = 0 \text{ the second term is zero)} \end{aligned}\right\} \quad \text{(A.3)}$$

or

$$F_1(\psi) = \frac{1}{\varepsilon}\left[\ln\psi\ln\frac{A_4}{A_3} + 2\ln\frac{1-\psi}{2\varepsilon\psi} - \ln(1-\xi^2)\right], \qquad \text{for } 1-\psi-\eta' = 0$$

* The work was performed in November, 1952, on a pilot model of the A.C.E. at N.P.L.

$$F_2(\psi) = \int_0^{1-\psi} \sum_{n=1}^{4} \frac{B_n(\bar{\eta})}{\rho_n(\bar{\eta})}\, d\bar{\eta} \,, \quad .. \quad .. \quad .. \quad .. \quad .. \quad .. \quad .. \quad .. \quad \text{(A.4)}$$

$$A_n = \rho_n(1-\psi) + X_n(1-\psi) \,, \quad .. \quad .. \quad .. \quad .. \quad .. \quad .. \quad .. \quad \text{(A.5)}$$

$$B_n = 1 + a_n Z_n - \frac{f_n + d_n(\bar{\eta} - \eta')}{g_n + \rho_n(\bar{\eta})} \,, \quad .. \quad .. \quad .. \quad .. \quad .. \quad .. \quad \text{(A.6)}$$

$$\left.\begin{aligned} Z_1 = Z_2 &= \frac{1}{\bar{\eta} - \eta'} \ln \frac{1-\bar{\eta}}{1-\eta'} \,, && \text{for } \bar{\eta} - \eta' \neq 0 \\ \text{or} \qquad &= -\frac{1}{1-\eta'} \,, && \text{for } \bar{\eta} - \eta' = 0 \\ Z_3 = Z_4 &= \frac{\ln(1-\bar{\eta})}{\bar{\eta} + \eta'} \,, && \text{for } \bar{\eta} + \eta' \neq 0 \\ \text{or} \qquad &= -1 && \text{for } \bar{\eta} = \eta' = 0 \end{aligned}\right\} \,, \quad .. \quad .. \quad .. \quad .. \quad \text{(A.7)}$$

$$\left.\begin{aligned} \rho_1^2(\bar{\eta}) &= X_1^2(\bar{\eta}) + (\bar{\eta} - \eta')^2 \\ \rho_2^2(\bar{\eta}) &= X_2^2(\bar{\eta}) + (\bar{\eta} - \eta')^2 \\ \rho_3^2(\bar{\eta}) &= \rho_1^2(\bar{\eta}) + 4\bar{\eta}\eta' \\ \rho_4^2(\bar{\eta}) &= \rho_2^2(\bar{\eta}) + 4\bar{\eta}\eta' \end{aligned}\right\} \,, \quad .. \quad .. \quad .. \quad .. \quad .. \quad .. \quad \text{(A.8)}$$

$$\left.\begin{aligned} X_1(\bar{\eta}) = X_3(\bar{\eta}) &= b_1(\bar{\eta} - \eta') + g_1 \\ X_2(\bar{\eta}) = X_4(\bar{\eta}) &= b_2(\bar{\eta} - \eta') - g_2 \end{aligned}\right| \,, \quad .. \quad .. \quad .. \quad .. \quad .. \quad .. \quad \text{(A.9)}$$

$$g_1 = a_1\varepsilon \,, \quad g_2 = a_2\varepsilon \,, \quad g_3 = g_4 = 0 \,, \quad .. \quad .. \quad .. \quad .. \quad .. \quad .. \quad \text{A.10)}$$

$$f_1 = 2a_1b_1 \ln(1-\eta') \,, \quad f_2 = -2a_2b_2 \ln(1-\eta') \,, \quad f_3 = f_4 = 0 \,, \quad .. \quad .. \quad \text{(A.11)}$$

$$d_1 = \frac{1 + b_1^2}{\varepsilon} \ln(1-\eta') \,, \quad d_2 = \frac{1 + b_2^2}{\varepsilon} \ln(1-\eta') \,, \quad d_3 = d_4 = 0 \,, \quad .. \quad \text{(A.12)}$$

$$a_1 = (1-\eta')(1+\xi) \,, \quad a_2 = (1-\eta')(1-\xi) \,,$$
$$a_3 = a_1 - 2\eta'(K-1) \,, \quad a_4 = a_2 + 2\eta'(K+1) \,, \quad .. \quad .. \quad .. \quad .. \quad \text{(A.13)}$$

$$b_1 = (K-1)\varepsilon \,, \quad b_2 = (K+1)\varepsilon \,. \quad .. \quad .. \quad .. \quad .. \quad .. \quad .. \quad \text{(A.14)}$$

3. The programme was made as simple and repetitive as possible, and no attempt was made to take advantage of the simplification arising when, for example, $K = 0$ or $\xi = 0$. In fact, it will be noticed that the term $\{f + c(\bar{\eta} - \eta')\}/(g + \rho)$ (with zero coefficients) was deliberately introduced into B_3 and B_4 in order that all B's were computed in the same way. Thus, although the computation took longer, the number of different instructions to be stored in the machine was reduced to a minimum. Even so, it was completely impossible to load the whole problem into the machine at one time, and it was broken down into three main parts (each sufficient to fill completely the storage space available). These were :

(*a*) The computation of all quantities not involving $\bar{\eta}$ and ψ and defined by equations (A.10) to (A.14).

(*b*) The computation and accumulation of successive values of $\Sigma\, B/\rho$ by application of equations (A.6) to (A.9)

(*c*) The completion of the computation by application of equations (A.2) to (A.5).

This break-down into three main programmes could have been effected in either of two ways:

(i) Completing one problem at a time by changing the programmes (many copies of which are required) as necessary, and not punching any intermediate results, only the final result

(ii) Completing each part of the computation in turn for all problems, punching out all intermediate results.

The method (i) was at first adopted but, owing to the difficulty of performing some of the integrations, a compromise was forced for the larger values of η' and ξ. This led to the punching and need for the efficient filing of some 14,000 cards bearing intermediate results, whereas all the final results occupy only 2,000 cards. (A rough estimate of the number of cards which would have been punched if the computation had been performed on standard Hollerith machines is one-third of a million.)

4. At first the integration was performed using Simpson's rule, each value of the integrand being added, as formed, with ' weights ' 2 or 4 to a running total, the integral being finally corrected by adjusting the end ' weights '. The process was checked by repeating at half the interval of integration (for the smallest ε only or for increasing ε until agreement was reached). For larger values of ξ and η' and the smaller values of ε, the integration was performed at half the basic interval and checked by halving again.

If the process had been continued as ξ and η' were further increased the interval would have become so small that the process would have become impossibly slow. At the time when this threatened the machine was increased in size by the addition of one more long delay line, offering storage space for 32 more instructions. This enabled:

(a) a more powerful integration formula to be used

(b) the interval to be varied, being large over by far the greatest part of the range, and progressively reduced as the more troublesome part (near $\bar{\eta} = \eta'$) was approached.

The interval was not controlled automatically by the behaviour of the integrand but all intervals were fixed upon prior examination of the function in the worst cases $\varepsilon = 0{\cdot}2$, $|\xi| = 0{\cdot}8$. Variations of the programmes were constructed for each value of η'.

When integrating using Simpson's rule only the final values were punched out, for the remainder of the work the integrand values were punched out (in binary form, twelve for each card) and integrated subsequently using a separate programme.

5. The values of the various parameters were originally fixed as:

$\psi = 0,\ 0{\cdot}15,\ 0{\cdot}30$ and $0{\cdot}45$

ε, various simple decimal values, mainly multiples of $0{\cdot}1$ but with $0{\cdot}25$ and $0{\cdot}75$ added

$\xi = -\ 0{\cdot}8(0{\cdot}2) + 0{\cdot}8$

$\eta' = 0(0{\cdot}1)1 - \psi$ with occasional extra values such as $0{\cdot}65$, $0{\cdot}85$.

There are several points in the computation where there are alternative procedures depending upon whether $\bar{\eta} - \eta' = 0$ or $\neq 0$. The A.C.E. being a binary machine, 1/10 is not exactly represented, and so η' (read in initially) and $\bar{\eta}$ (built up as a multiple of a rounded off $\delta\bar{\eta}$) would never exactly agree. This would lead to (for example) the computation of the nearly indeterminate form:

$$Z_1 = \frac{1}{\bar{\eta} - \eta'} \ln \frac{1 - \bar{\eta}}{1 - \eta'},$$

where $(\bar{\eta} - \eta')$ was simply the accumulation of rounding errors where the alternative form of equation A.7 namely $Z_1 = -1/1 - \eta'$ should be used. Two ways out of this are possible:

(*a*) Using a scale factor $S(S = 10^p 2^q)$ such that $S\,\delta\bar{\eta}$ is exact

(*b*) To discriminate not on $(\bar{\eta} - \eta')$ being zero but being less than some assigned quantity.

Both of these procedures require extra instructions and, as we have seen, it was imperative to keep demands on storage space to a minimum. Accordingly, enquiries were made if the interval of η' could be 1/8 instead of 1/10 and if ψ could take the values (near 0·15, 0·3 and 0·45) 1/8, 5/16 and 7/16. This was readily agreed.

Further, it is clear that the supervelocity for $\psi = 0$ would have to be computed by some quite different programme. From physical considerations the differences between ψ being zero and having some small value are quite negligible except at the wing tip. Again it was readily agreed to substitute 1/16 for $\psi = 0$.

There was no difficulty with decimal values of ξ, each computation being independent. The remaining parameter, ε, took values $0{\cdot}2(0{\cdot}1)1{\cdot}0$ and was built up by the machine from $\delta\varepsilon$ and so there is an accumulation of error. The largest error is, however, only 4×10^{-6} and so completely negligible.

6. The supervelocity is a smoother function of ε than of either ξ or η' and the most powerful differencing check is with respect to ε. This is somewhat unfortunate in that two values of ε were computed within minutes of each other whereas two values of ξ or η' were computed days or even weeks apart, and so differencing with respect to these latter would be a slightly better check on the behaviour of the machine.

The results were differenced with respect to ε using a Hollerith Tabulator. Some of the questionable values were recomputed but in many cases the correct value could be ' run in '.

Differencing with respect to η' was not carried out systematically because of those values not conforming to the constant interval. Some differencing (for $\varepsilon = 0{\cdot}2$) was done, ignoring these odd values of η'. The supervelocity is a smooth function of η' except near the wing root and wing tip where the differences were more often exceptionally large. Only 9 values of ξ were computed and Δ^8_ξ is not in general negligible.

However, except at the wing tips, $\Delta\eta$ is a smooth function of ξ, and Δ^4_{η',ξ^3} is, in general, negligible. This was found for $\varepsilon = 0{\cdot}2$

Apart from the wing-tip values we have adequate differencing checks. However, these are smooth functions of ψ and in many cases almost independent of ψ. The table illustrates this:

Swept-back wing, $\xi = 0$, $\eta' = 1 - \psi$

ε \ ψ =	0·4375	0·3125	0·125	0·0625
0·2	0·481	0·483	0·488	0·488
0·3	0·439	0·437	0·440	0·436
0·4	0·393	0·387	0·379	0·375
0·5	0·351	0·340	0·325	0·318
0·6	0·313	0·298	0·278	0·269
0·7	0·280	0·262	0·238	0·227
0·8	0·251	0·231	0·205	0·193
0·9	0·226	0·204	0·177	0·164
1·0	0·204	0·181	0·154	0·141

7. The final printed copy was prepared by the card-operated Electromatic typewriter, and checked as follows. The cards were summed in small groups on a Hollerith Tabulator and the sums compared with corresponding sums formed from the printed copy using desk machine. A few typing errors were found and corrected; also a few errors of loading the cards in the typewriter.

8. All computation was carried out to 20 binary places, equivalent to 6 decimals and finally rounded off to 3 decimals. The results are not guaranteed to three decimals but errors should not exceed 1 unit.

9. The time taken was approximately 150 hours. The efficiency was not high partly owing to the difficulties imposed by the large demand on storage space. It is roughly estimated that the computation was done at about 60 to 70 times as fast as it would have been on desk machines, whereas this factor is more commonly of the order of 200 to 300.

10. The work described in this Appendix was carried out on the Automatic Computing Engine at the National Physical Laboratory, and the Appendix is published by permission of the Director, N.P.L.

TABLE 1

Supervelocities along Mid-chord lines of Cropped Rhombus Wings with Taper Ratios $\psi = 0{\cdot}0625, 0{\cdot}1250, 0{\cdot}3125$ *and* $0{\cdot}4375$ *and Convergence Ratios* $\varepsilon = 0{\cdot}2(0{\cdot}1)1{\cdot}0$, *tabulated for* η' *from* 0 *to* $(1 - \psi)$ *at Various Intervals*

		$\varepsilon =$	0·2	0·3	0·4	0·5	0·6	0·7	0·8	0·9	1·0
ψ	η'										
0·0625	0·0000		0·925	0·897	0·872	0·850	0·830	0·811	0·794	0·779	0·764
	0·1250		0·956	0·926	0·899	0·875	0·853	0·833	0·815	0·798	0·782
	0·2500		0·980	0·959	0·935	0·912	0·890	0·869	0·850	0·832	0·816
	0·3750		0·995	0·982	0·965	0·947	0·927	0·908	0·890	0·872	0·855
	0·5000		1·004	0·999	0·990	0·978	0·963	0·947	0·931	0·915	0·899
	0·5625		1·007	1·006	1·001	0·992	0·980	0·966	0·952	0·938	0·923
	0·6250		1·010	1·013	1·011	1·005	0·997	0·986	0·974	0·961	0·947
	0·6875		1·014	1·019	1·021	1·019	1·014	1·006	0·997	0·986	0·974
	0·7500		1·018	1·025	1·032	1·034	1·032	1·028	1·021	1·013	1·003
	0·8750		1·023	1·038	1·052	1·062	1·069	1·072	1·071	1·068	1·062
	0·9375		0·568	0·605	0·641	0·673	0·702	0·726	0·745	0·760	0·772
0·1250	0·0000		0·925	0·897	0·872	0·850	0·830	0·811	0·794	0·779	0·764
	0·1250		0·956	0·926	0·899	0·875	0·853	0·833	0·814	0·797	0·782
	0·2500		0·980	0·958	0·935	0·912	0·890	0·869	0·850	0·832	0·816
	0·3750		0·995	0·982	0·965	0·946	0·927	0·908	0·889	0·872	0·855
	0·5000		1·003	0·999	0·989	0·977	0·962	0·946	0·930	0·914	0·898
	0·5625		1·007	1·006	1·000	0·991	0·979	0·965	0·951	0·936	0·920
	0·6250		1·009	1·013	1·010	1·004	0·995	0·984	0·971	0·957	0·943
	0·6875		1·013	1·018	1·019	1·017	1·010	1·002	0·991	0·979	0·965
	0·7500		1·010	1·022	1·027	1·027	1·023	1·016	1·007	0·995	0·983
	0·8750		0·562	0·593	0·621	0·645	0·664	0·679	0·690	0·697	0·702
0·3125	0·0000		0·925	0·896	0·871	0·848	0·827	0·808	0·790	0·773	0·757
	0·1250		0·956	0·925	0·898	0·873	0·850	0·829	0·809	0·791	0·774
	0·2500		0·980	0·957	0·933	0·908	0·885	0·863	0·842	0·822	0·804
	0·3750		0·993	0·979	0·960	0·939	0·917	0·895	0·873	0·853	0·833
	0·5000		0·999	0·989	0·974	0·955	0·934	0·911	0·888	0·867	0·845
	0·5625		0·996	0·984	0·966	0·945	0·922	0·899	0·876	0·853	0·831
	0·6250		0·966	0·941	0·914	0·889	0·865	0·842	0·820	0·800	0·780
	0·6875		0·551	0·571	0·585	0·594	0·599	0·601	0·600	0·596	0·592
0·4375	0·0000		0·924	0·894	0·867	0·842	0·819	0·797	0·776	0·757	0·738
	0·1250		0·954	0·923	0·893	0·865	0·840	0·816	0·793	0·772	0·752
	0·2500		0·977	0·952	0·923	0·895	0·867	0·841	0·816	0·792	0·770
	0·3750		0·984	0·962	0·934	0·904	0·874	0·845	0·818	0·792	0·768
	0·5000		0·931	0·889	0·851	0·819	0·789	0·762	0·737	0·715	0·693
	0·5625		0·545	0·558	0·564	0·566	0·564	0·560	0·554	0·546	0·538

(71240) Wt. 52/8943 K.7 10/58 Hw.

PRINTED IN GREAT BRITAIN

TABLE 2

Supervelocities over cropped arrowhead wings for varying taper ratio ψ, convergence ratio ϵ, co-ordinate ξ and η'

$\psi = 0{\cdot}0625$

ϵ	η' \ ξ	-0.8	-0.6	-0.4	-0.2	0.0	+0.2	+0.4	+0.6	+0.8
0.2	0.0000	0.323	0.693	0.850	0.890	0.843	0.718	0.513	0.203	-0.287
	0.1250	0.112	0.548	0.770	0.877	0.898	0.844	0.712	0.481	0.076
	0.2500	0.091	0.525	0.752	0.867	0.900	0.860	0.742	0.525	0.130
	0.3750	0.086	0.521	0.749	0.865	0.901	0.864	0.749	0.536	0.144
	0.5000	0.085	0.520	0.748	0.866	0.902	0.866	0.752	0.540	0.150
	0.5625	0.085	0.520	0.749	0.866	0.902	0.866	0.753	0.541	0.151
	0.6250	0.085	0.521	0.749	0.867	0.902	0.867	0.754	0.542	0.153
	0.6875	0.086	0.521	0.749	0.867	0.904	0.868	0.755	0.544	0.154
	0.7500	0.088	0.522	0.750	0.868	0.905	0.869	0.756	0.544	0.155
	0.8750	0.086	0.523	0.752	0.870	0.907	0.870	0.758	0.547	0.157
	0.9375	-0.073	0.180	0.329	0.428	0.488	0.512	0.504	0.446	0.307
0.3	0.0000	0.390	0.708	0.822	0.826	0.751	0.606	0.390	0.088	0.370
	0.1250	0.122	0.537	0.742	0.829	0.832	0.764	0.627	0.406	0.039
	0.2500	0.079	0.487	0.697	0.802	0.828	0.787	0.676	0.480	0.133
	0.3750	0.065	0.472	0.682	0.789	0.819	0.785	0.683	0.495	0.157
	0.5000	0.059	0.466	0.676	0.783	0.816	0.782	0.682	0.497	0.162
	0.5625	0.056	0.464	0.673	0.782	0.813	0.781	0.681	0.497	0.163
	0.6250	0.055	0.462	0.673	0.780	0.813	0.780	0.681	0.497	0.163
	0.6875	0.054	0.461	0.672	0.780	0.812	0.780	0.680	0.497	0.162
	0.7500	0.053	0.461	0.672	0.779	0.812	0.779	0.680	0.497	0.163
	0.8750	0.051	0.458	0.670	0.778	0.815	0.779	0.680	0.497	0.162
	0.9375	-0.144	0.105	0.260	0.365	0.436	0.475	0.485	0.451	0.349
0.4	0.0000	0.436	0.704	0.783	0.760	0.667	0.513	0.299	0.012	-0.404
	0.1250	0.132	0.529	0.715	0.783	0.769	0.691	0.552	0.342	0.010
	0.2500	0.071	0.452	0.648	0.743	0.765	0.723	0.619	0.440	0.133
	0.3750	0.048	0.426	0.619	0.716	0.744	0.714	0.623	0.460	0.168
	0.5000	0.036	0.413	0.606	0.702	0.731	0.701	0.615	0.456	0.170
	0.5625	0.032	0.409	0.601	0.698	0.727	0.695	0.612	0.453	0.168
	0.6250	0.029	0.405	0.598	0.694	0.723	0.695	0.609	0.451	0.166
	0.6875	0.026	0.402	0.595	0.691	0.720	0.692	0.606	0.448	0.163
	0.7500	0.024	0.400	0.592	0.689	0.718	0.689	0.603	0.446	0.161
	0.8750	0.016	0.393	0.586	0.684	0.713	0.685	0.599	0.441	0.160
	0.9375	-0.206	0.038	0.192	0.300	0.375	0.424	0.445	0.430	0.353
0.5	0.0000	0.465	0.690	0.740	0.699	0.595	0.439	0.232	-0.037	-0.414
	0.1250	0.139	0.520	0.689	0.739	0.713	0.627	0.489	0.290	-0.011
	0.2500	0.063	0.420	0.604	0.694	0.712	0.670	0.572	0.407	0.131
	0.3750	0.034	0.383	0.562	0.652	0.679	0.654	0.574	0.431	0.177
	0.5000	0.019	0.365	0.541	0.629	0.657	0.633	0.558	0.421	0.175
	0.5625	0.013	0.359	0.534	0.622	0.650	0.622	0.550	0.414	0.169
	0.6250	0.008	0.354	0.529	0.616	0.643	0.619	0.544	0.408	0.163
	0.6875	0.003	0.349	0.524	0.611	0.637	0.613	0.539	0.402	0.157
	0.7500	-0.000	0.345	0.519	0.606	0.633	0.608	0.534	0.397	0.153
	0.8750	-0.012	0.335	0.511	0.597	0.624	0.600	0.525	0.389	0.146
	0.9375	-0.249	-0.017	0.133	0.240	0.318	0.372	0.401	0.398	0.341
0.6	0.0000	0.481	0.669	0.698	0.644	0.535	0.381	0.183	-0.069	-0.411
	0.1250	0.143	0.511	0.663	0.698	0.662	0.573	0.438	0.250	-0.025
	0.2500	0.055	0.391	0.566	0.651	0.667	0.625	0.532	0.378	0.129
	0.3750	0.023	0.345	0.511	0.596	0.624	0.604	0.536	0.408	0.183
	0.5000	0.005	0.323	0.485	0.566	0.592	0.575	0.509	0.391	0.177
	0.5625	-0.002	0.316	0.476	0.555	0.583	0.561	0.498	0.380	0.167
	0.6250	-0.008	0.309	0.469	0.548	0.575	0.553	0.488	0.370	0.158
	0.6875	-0.014	0.304	0.462	0.541	0.566	0.545	0.480	0.361	0.148
	0.7500	-0.019	0.298	0.456	0.535	0.559	0.538	0.473	0.354	0.142
	0.8750	-0.032	0.286	0.445	0.524	0.548	0.566	0.460	0.341	0.127
	0.9375	-0.278	-0.059	0.086	0.191	0.269	0.324	0.358	0.364	0.321
0.7	0.0000	0.488	0.646	0.658	0.596	0.484	0.334	0.146	-0.089	-0.402
	0.1250	0.145	0.501	0.637	0.660	0.617	0.527	0.395	0.218	-0.036
	0.2500	0.047	0.364	0.533	0.615	0.629	0.587	0.496	0.354	0.125
	0.3750	0.013	0.312	0.467	0.548	0.578	0.562	0.505	0.389	0.188
	0.5000	-0.006	0.287	0.435	0.511	0.536	0.526	0.468	0.365	0.179
	0.5625	-0.013	0.278	0.425	0.498	0.525	0.510	0.453	0.350	0.164
	0.6250	-0.020	0.271	0.417	0.490	0.519	0.497	0.439	0.337	0.151
	0.6875	-0.027	0.265	0.409	0.482	0.504	0.487	0.429	0.326	0.138
	0.7500	-0.032	0.258	0.403	0.474	0.497	0.478	0.421	0.317	0.130
	0.8750	-0.047	0.245	0.391	0.462	0.483	0.464	0.406	0.301	0.111
	0.9375	-0.298	-0.090	0.048	0.150	0.227	0.283	0.319	0.331	0.301
0.8	0.0000	0.489	0.622	0.621	0.553	0.442	0.296	0.118	-0.102	-0.390
	0.1250	0.146	0.491	0.613	0.626	0.578	0.487	0.360	0.192	-0.043
	0.2500	0.040	0.339	0.504	0.584	0.596	0.555	0.467	0.332	0.121
	0.3750	0.005	0.282	0.428	0.507	0.539	0.527	0.479	0.373	0.191
	0.5000	-0.015	0.256	0.393	0.464	0.488	0.483	0.433	0.344	0.179
	0.5625	-0.022	0.246	0.382	0.449	0.474	0.467	0.414	0.324	0.157
	0.6250	-0.029	0.239	0.373	0.440	0.471	0.450	0.398	0.308	0.144
	0.6875	-0.036	0.233	0.364	0.431	0.452	0.437	0.386	0.294	0.127
	0.7500	-0.042	0.225	0.358	0.423	0.444	0.428	0.377	0.284	0.118
	0.8750	-0.056	0.212	0.345	0.409	0.429	0.412	0.360	0.266	0.097
	0.9375	-0.313	-0.113	0.019	0.117	0.193	0.249	0.286	0.302	0.279
0.9	0.0000	0.486	0.598	0.587	0.516	0.406	0.266	0.096	-0.110	-0.377
	0.1250	0.145	0.481	0.589	0.594	0.543	0.453	0.330	0.171	-0.047
	0.2500	0.033	0.317	0.479	0.557	0.567	0.526	0.441	0.313	0.117
	0.3750	-0.002	0.256	0.393	0.471	0.506	0.498	0.458	0.359	0.192
	0.5000	-0.022	0.228	0.356	0.423	0.446	0.446	0.403	0.325	0.179
	0.5625	-0.029	0.219	0.344	0.406	0.430	0.431	0.381	0.302	0.148
	0.6250	-0.036	0.212	0.335	0.397	0.430	0.409	0.362	0.283	0.136
	0.6875	-0.043	0.206	0.326	0.388	0.408	0.395	0.349	0.267	0.118
	0.7500	-0.049	0.197	0.319	0.380	0.399	0.385	0.339	0.256	0.107
	0.8750	-0.063	0.185	0.307	0.365	0.383	0.368	0.321	0.236	0.086
	0.9375	-0.319	-0.130	-0.003	0.091	0.164	0.220	0.258	0.276	0.259
1.0	0.0000	0.480	0.575	0.556	0.484	0.375	0.240	0.079	-0.115	-0.364
	0.1250	0.144	0.471	0.567	0.566	0.512	0.423	0.304	0.153	-0.051
	0.2500	0.027	0.298	0.457	0.534	0.541	0.500	0.417	0.296	0.113
	0.3750	-0.008	0.233	0.363	0.439	0.477	0.473	0.439	0.347	0.192
	0.5000	-0.028	0.205	0.324	0.388	0.410	0.414	0.377	0.313	0.178
	0.5625	-0.035	0.196	0.312	0.370	0.392	0.401	0.354	0.282	0.153
	0.6250	-0.042	0.189	0.302	0.361	0.395	0.374	0.331	0.261	0.129
	0.6875	-0.049	0.183	0.293	0.351	0.370	0.358	0.317	0.243	0.109
	0.7500	-0.054	0.174	0.287	0.342	0.360	0.348	0.307	0.232	0.097
	0.8750	-0.067	0.163	0.275	0.328	0.345	0.331	0.290	0.211	0.074
	0.9375	-0.322	-0.142	-0.021	0.070	0.141	0.195	0.234	0.253	0.241

TABLE 2 *continued*

Supervelocities over cropped arrowhead wings for varying taper ratio ψ, convergence ratio ϵ, co-ordinate ξ and y'

$\psi = 0{\cdot}1250$

ϵ	y'	ξ -0.8	-0.6	-0.4	-0.2	0.0	+0.2	+0.4	+0.6	+0.8
0.2	0.0000	0.323	0.693	0.850	0.890	0.843	0.718	0.513	0.203	-0.287
	0.1250	0.112	0.547	0.770	0.877	0.898	0.844	0.712	0.481	0.076
	0.2500	0.091	0.525	0.752	0.867	0.900	0.860	0.742	0.525	0.130
	0.3750	0.086	0.521	0.749	0.865	0.900	0.863	0.749	0.536	0.144
	0.5000	0.085	0.520	0.748	0.866	0.902	0.866	0.752	0.540	0.150
	0.5625	0.085	0.520	0.749	0.866	0.902	0.866	0.753	0.541	0.151
	0.6250	0.085	0.521	0.749	0.867	0.902	0.867	0.754	0.542	0.153
	0.6875	0.086	0.521	0.749	0.867	0.904	0.868	0.755	0.544	0.154
	0.7500	0.087	0.521	0.750	0.868	0.904	0.868	0.756	0.544	0.155
	0.8750	-0.074	0.177	0.328	0.426	0.488	0.511	0.502	0.444	0.304
0.3	0.0000	0.390	0.708	0.822	0.826	0.750	0.606	0.390	0.087	-0.370
	0.1250	0.122	0.537	0.742	0.829	0.832	0.764	0.626	0.406	0.039
	0.2500	0.079	0.487	0.697	0.802	0.828	0.787	0.676	0.480	0.133
	0.3750	0.065	0.472	0.682	0.789	0.819	0.785	0.683	0.495	0.157
	0.5000	0.059	0.466	0.676	0.783	0.816	0.782	0.682	0.497	0.162
	0.5625	0.056	0.464	0.673	0.781	0.813	0.781	0.681	0.497	0.163
	0.6250	0.055	0.462	0.673	0.780	0.813	0.780	0.681	0.497	0.163
	0.6875	0.053	0.461	0.672	0.780	0.812	0.780	0.681	0.497	0.163
	0.7500	0.051	0.460	0.671	0.779	0.812	0.780	0.681	0.497	0.163
	0.8750	-0.143	0.106	0.260	0.365	0.440	0.476	0.485	0.453	0.349
0.4	0.0000	0.436	0.704	0.783	0.760	0.667	0.513	0.299	0.012	-0.404
	0.1250	0.132	0.529	0.715	0.783	0.769	0.691	0.552	0.342	0.010
	0.2500	0.071	0.452	0.648	0.743	0.765	0.723	0.619	0.440	0.133
	0.3750	0.048	0.426	0.619	0.716	0.744	0.714	0.623	0.460	0.168
	0.5000	0.036	0.413	0.606	0.702	0.731	0.701	0.615	0.456	0.170
	0.5625	0.032	0.409	0.601	0.698	0.727	0.695	0.612	0.453	0.168
	0.6250	0.029	0.405	0.598	0.694	0.724	0.695	0.609	0.451	0.166
	0.6875	0.025	0.402	0.595	0.692	0.721	0.692	0.606	0.448	0.164
	0.7500	0.022	0.399	0.592	0.689	0.719	0.690	0.604	0.447	0.162
	0.8750	-0.201	0.042	0.195	0.303	0.379	0.428	0.449	0.435	0.357
0.5	0.0000	0.465	0.690	0.740	0.699	0.595	0.439	0.232	-0.037	-0.414
	0.1250	0.139	0.520	0.689	0.739	0.713	0.627	0.489	0.290	-0.011
	0.2500	0.063	0.420	0.604	0.694	0.712	0.670	0.572	0.407	0.131
	0.3750	0.034	0.383	0.562	0.652	0.679	0.654	0.574	0.431	0.177
	0.5000	0.019	0.365	0.541	0.629	0.657	0.633	0.558	0.421	0.175
	0.5625	0.013	0.359	0.535	0.622	0.650	0.622	0.550	0.414	0.169
	0.6250	0.008	0.354	0.529	0.616	0.643	0.619	0.544	0.408	0.163
	0.6875	0.003	0.349	0.525	0.611	0.638	0.614	0.539	0.402	0.157
	0.7500	-0.002	0.344	0.520	0.608	0.634	0.610	0.535	0.399	0.154
	0.8750	-0.242	-0.010	0.140	0.247	0.325	0.379	0.408	0.406	0.349
0.6	0.0000	0.481	0.669	0.698	0.644	0.535	0.381	0.183	-0.069	-0.411
	0.1250	0.143	0.511	0.663	0.698	0.662	0.573	0.438	0.250	-0.025
	0.2500	0.055	0.391	0.566	0.651	0.667	0.625	0.532	0.378	0.129
	0.3750	0.023	0.345	0.511	0.596	0.624	0.604	0.536	0.408	0.183
	0.5000	0.005	0.323	0.485	0.566	0.592	0.575	0.509	0.391	0.177
	0.5625	-0.002	0.316	0.476	0.556	0.583	0.561	0.498	0.380	0.167
	0.6250	-0.008	0.309	0.469	0.548	0.575	0.553	0.488	0.370	0.158
	0.6875	-0.014	0.304	0.463	0.542	0.566	0.546	0.480	0.362	0.148
	0.7500	-0.020	0.298	0.458	0.537	0.561	0.540	0.475	0.356	0.143
	0.8750	-0.271	-0.049	0.095	0.200	0.278	0.334	0.368	0.374	0.332
0.7	0.0000	0.488	0.646	0.658	0.596	0.484	0.334	0.146	-0.089	-0.402
	0.1250	0.145	0.501	0.637	0.660	0.617	0.527	0.395	0.218	-0.036
	0.2500	0.047	0.364	0.533	0.615	0.629	0.587	0.497	0.354	0.125
	0.3750	0.013	0.312	0.467	0.548	0.578	0.562	0.505	0.389	0.188
	0.5000	-0.006	0.287	0.435	0.511	0.536	0.526	0.468	0.365	0.179
	0.5625	-0.013	0.279	0.425	0.498	0.525	0.510	0.453	0.350	0.164
	0.6250	-0.020	0.271	0.417	0.490	0.519	0.497	0.440	0.337	0.151
	0.6875	-0.026	0.266	0.410	0.482	0.505	0.487	0.430	0.326	0.138
	0.7500	-0.033	0.260	0.405	0.477	0.499	0.480	0.423	0.318	0.131
	0.8750	-0.290	-0.079	0.059	0.161	0.238	0.295	0.331	0.343	0.312
0.8	0.0000	0.489	0.622	0.621	0.553	0.442	0.296	0.118	-0.102	-0.390
	0.1250	0.146	0.491	0.613	0.626	0.578	0.487	0.360	0.192	-0.043
	0.2500	0.040	0.339	0.504	0.584	0.596	0.555	0.467	0.332	0.121
	0.3750	0.005	0.282	0.428	0.507	0.539	0.528	0.479	0.373	0.191
	0.5000	-0.015	0.256	0.393	0.464	0.488	0.483	0.433	0.344	0.179
	0.5625	-0.022	0.247	0.382	0.449	0.475	0.467	0.414	0.324	0.158
	0.6250	-0.029	0.239	0.373	0.440	0.472	0.450	0.398	0.308	0.144
	0.6875	-0.035	0.234	0.365	0.432	0.453	0.438	0.387	0.295	0.128
	0.7500	-0.041	0.228	0.361	0.426	0.446	0.430	0.379	0.286	0.119
	0.8750	-0.301	-0.102	0.031	0.130	0.205	0.261	0.299	0.315	0.292
0.9	0.0000	0.486	0.598	0.587	0.516	0.406	0.266	0.096	-0.110	-0.377
	0.1250	0.145	0.481	0.589	0.594	0.543	0.453	0.330	0.171	-0.047
	0.2500	0.033	0.318	0.479	0.557	0.567	0.526	0.441	0.313	0.117
	0.3750	-0.002	0.256	0.394	0.471	0.506	0.498	0.458	0.359	0.192
	0.5000	-0.022	0.229	0.356	0.423	0.446	0.446	0.403	0.325	0.179
	0.5625	-0.029	0.220	0.344	0.407	0.430	0.432	0.381	0.302	0.150
	0.6250	-0.036	0.211	0.335	0.398	0.431	0.409	0.362	0.283	0.136
	0.6875	-0.042	0.207	0.327	0.389	0.409	0.396	0.349	0.268	0.118
	0.7500	-0.047	0.201	0.323	0.383	0.401	0.387	0.341	0.258	0.108
	0.8750	-0.307	-0.118	0.009	0.104	0.177	0.233	0.271	0.289	0.273
1.0	0.0000	0.480	0.575	0.557	0.484	0.376	0.240	0.079	-0.115	-0.364
	0.1250	0.144	0.471	0.574	0.566	0.512	0.423	0.304	0.153	-0.051
	0.2500	0.027	0.298	0.457	0.534	0.541	0.500	0.417	0.296	0.113
	0.3750	-0.008	0.233	0.364	0.439	0.477	0.473	0.439	0.347	0.192
	0.5000	-0.027	0.205	0.324	0.388	0.410	0.414	0.377	0.313	0.178
	0.5625	-0.035	0.196	0.312	0.370	0.392	0.401	0.354	0.282	0.153
	0.6250	-0.041	0.188	0.303	0.361	0.396	0.374	0.331	0.261	0.129
	0.6875	-0.047	0.184	0.294	0.352	0.370	0.359	0.317	0.244	0.109
	0.7500	-0.051	0.179	0.291	0.346	0.363	0.350	0.309	0.233	0.098
	0.8750	-0.309	-0.130	-0.008	0.083	0.154	0.209	0.248	0.267	0.255

TABLE 2 *continued*

Supervelocities over cropped arrowhead wings for varying taper ratio ψ, convergence ratio ϵ, co-ordinate ξ and η'

ψ = 0·3125

ϵ	η'	ξ -0.8	-0.6	-0.4	-0.2	0.0	+0.2	+0.4	+0.6	+0.8
0.2	0.0000	0.323	0.693	0.850	0.890	0.843	0.718	0.513	0.203	-0.287
	0.1250	0.112	0.547	0.770	0.877	0.898	0.844	0.711	0.481	0.076
	0.2500	0.090	0.525	0.751	0.867	0.900	0.859	0.742	0.525	0.130
	0.3750	0.085	0.520	0.748	0.865	0.900	0.863	0.748	0.536	0.144
	0.5000	0.081	0.517	0.746	0.864	0.900	0.865	0.752	0.540	0.150
	0.5625	0.074	0.510	0.741	0.860	0.898	0.864	0.753	0.542	0.153
	0.6250	0.047	0.480	0.710	0.835	0.882	0.857	0.754	0.548	0.162
	0.6875	-0.076	0.174	0.325	0.423	0.483	0.509	0.499	0.442	0.298
0.3	0.0000	0.390	0.707	0.822	0.826	0.750	0.606	0.390	0.088	-0.369
	0.1250	0.122	0.537	0.742	0.829	0.832	0.764	0.627	0.406	0.039
	0.2500	0.079	0.487	0.697	0.801	0.828	0.787	0.676	0.480	0.133
	0.3750	0.063	0.471	0.682	0.788	0.819	0.785	0.683	0.496	0.158
	0.5000	0.051	0.460	0.673	0.781	0.815	0.783	0.683	0.499	0.164
	0.5625	0.036	0.445	0.663	0.775	0.812	0.783	0.685	0.502	0.168
	0.6250	-0.006	0.396	0.614	0.738	0.792	0.781	0.696	0.518	0.183
	0.6875	-0.141	0.107	0.262	0.367	0.437	0.477	0.485	0.453	0.348
0.4	0.0000	0.436	0.704	0.783	0.761	0.667	0.513	0.299	0.012	-0.404
	0.1250	0.131	0.528	0.715	0.783	0.770	0.691	0.552	0.342	0.010
	0.2500	0.070	0.452	0.648	0.743	0.765	0.724	0.620	0.441	0.133
	0.3750	0.046	0.425	0.619	0.716	0.745	0.715	0.623	0.461	0.169
	0.5000	0.026	0.406	0.603	0.703	0.734	0.705	0.619	0.460	0.173
	0.5625	0.003	0.385	0.588	0.695	0.730	0.703	0.620	0.461	0.175
	0.6250	-0.051	0.321	0.527	0.648	0.709	0.708	0.638	0.481	0.190
	0.6875	-0.192	0.050	0.204	0.311	0.387	0.435	0.456	0.442	0.365
0.5	0.0000	0.465	0.690	0.740	0.699	0.595	0.439	0.233	-0.037	-0.414
	0.1250	0.138	0.520	0.689	0.739	0.713	0.628	0.490	0.291	-0.011
	0.2500	0.062	0.420	0.605	0.694	0.712	0.671	0.572	0.407	0.132
	0.3750	0.032	0.383	0.562	0.653	0.680	0.655	0.575	0.433	0.178
	0.5000	0.005	0.358	0.541	0.632	0.662	0.638	0.562	0.425	0.178
	0.5625	-0.024	0.332	0.522	0.624	0.660	0.634	0.562	0.422	0.176
	0.6250	-0.087	0.258	0.452	0.571	0.635	0.644	0.584	0.443	0.189
	0.6875	-0.229	0.004	0.154	0.261	0.340	0.393	0.422	0.421	0.365
0.6	0.0000	0.481	0.670	0.698	0.645	0.535	0.381	0.183	-0.068	-0.411
	0.1250	0.143	0.511	0.663	0.699	0.663	0.574	0.438	0.250	-0.025
	0.2500	0.055	0.391	0.567	0.652	0.668	0.626	0.532	0.379	0.129
	0.3750	0.021	0.346	0.513	0.598	0.626	0.606	0.537	0.410	0.184
	0.5000	-0.010	0.318	0.487	0.572	0.599	0.581	0.514	0.395	0.181
	0.5625	-0.045	0.286	0.465	0.562	0.598	0.576	0.510	0.390	0.175
	0.6250	-0.113	0.207	0.390	0.505	0.571	0.587	0.536	0.408	0.183
	0.6875	-0.254	-0.031	0.113	0.219	0.298	0.354	0.389	0.395	0.355
0.7	0.0000	0.488	0.647	0.658	0.596	0.485	0.335	0.147	-0.089	-0.401
	0.1250	0.146	0.502	0.638	0.661	0.618	0.527	0.396	0.218	-0.035
	0.2500	0.048	0.365	0.534	0.616	0.630	0.588	0.498	0.354	0.126
	0.3750	0.012	0.313	0.469	0.551	0.580	0.564	0.506	0.391	0.189
	0.5000	-0.023	0.283	0.440	0.519	0.544	0.533	0.473	0.370	0.182
	0.5625	-0.061	0.248	0.417	0.509	0.544	0.527	0.466	0.360	0.172
	0.6250	-0.132	0.166	0.339	0.450	0.517	0.537	0.493	0.375	0.175
	0.6875	-0.271	-0.058	0.080	0.184	0.262	0.319	0.357	0.370	0.340
0.8	0.0000	0.490	0.623	0.621	0.554	0.443	0.297	0.118	-0.102	-0.390
	0.1250	0.147	0.492	0.614	0.627	0.579	0.488	0.360	0.192	-0.042
	0.2500	0.041	0.341	0.506	0.586	0.597	0.556	0.468	0.333	0.122
	0.3750	0.005	0.285	0.431	0.510	0.542	0.530	0.481	0.375	0.192
	0.5000	-0.032	0.253	0.400	0.474	0.497	0.490	0.439	0.348	0.182
	0.5625	-0.073	0.216	0.376	0.464	0.497	0.486	0.428	0.334	0.167
	0.6250	-0.145	0.133	0.296	0.404	0.470	0.494	0.455	0.345	0.166
	0.6875	-0.281	-0.079	0.053	0.154	0.231	0.289	0.328	0.345	0.324
0.9	0.0000	0.487	0.599	0.588	0.517	0.407	0.266	0.096	-0.110	-0.376
	0.1250	0.147	0.482	0.591	0.595	0.544	0.453	0.330	0.171	-0.047
	0.2500	0.035	0.319	0.481	0.559	0.568	0.527	0.442	0.314	0.118
	0.3750	-0.001	0.260	0.397	0.474	0.508	0.500	0.459	0.361	0.193
	0.5000	-0.039	0.228	0.366	0.436	0.456	0.454	0.409	0.329	0.182
	0.5625	-0.082	0.189	0.341	0.425	0.456	0.451	0.394	0.311	0.164
	0.6250	-0.155	0.106	0.261	0.364	0.431	0.457	0.422	0.319	0.157
	0.6875	-0.287	-0.094	0.032	0.130	0.204	0.262	0.302	0.322	0.308
1.0	0.0000	0.481	0.576	0.557	0.484	0.376	0.241	0.079	-0.114	-0.363
	0.1250	0.146	0.472	0.569	0.567	0.513	0.423	0.305	0.154	-0.050
	0.2500	0.029	0.300	0.459	0.535	0.543	0.501	0.418	0.297	0.113
	0.3750	-0.006	0.238	0.368	0.443	0.480	0.475	0.441	0.348	0.194
	0.5000	-0.044	0.206	0.336	0.402	0.420	0.421	0.383	0.317	0.181
	0.5625	-0.088	0.167	0.311	0.391	0.420	0.421	0.362	0.291	0.159
	0.6250	-0.161	0.084	0.231	0.330	0.396	0.424	0.392	0.295	0.149
	0.6875	-0.289	-0.105	0.014	0.109	0.181	0.238	0.279	0.301	0.292

TABLE 2 *continued*

Supervelocities over cropped arrowhead wings for varying taper ratio ψ *, convergence ratio* ϵ *, co-ordinate* ξ *and* η'

ψ = 0·4375

ϵ	η' \ ξ	-0.8	-0.6	-0.4	-0.2	0.0	+0.2	+0.4	+0.6	+0.8
0.2	0.0000	0.322	0.692	0.849	0.889	0.842	0.718	0.513	0.203	-0.287
	0.1250	0.111	0.546	0.769	0.876	0.897	0.843	0.711	0.481	0.076
	0.2500	0.088	0.523	0.750	0.865	0.899	0.859	0.742	0.525	0.130
	0.3750	0.077	0.512	0.742	0.860	0.897	0.862	0.748	0.536	0.145
	0.5000	0.029	0.453	0.680	0.807	0.859	0.844	0.750	0.552	0.168
	0.5625	-0.078	0.174	0.324	0.421	0.481	0.507	0.497	0.439	0.294
0.3	0.0000	0.389	0.706	0.821	0.826	0.751	0.606	0.391	0.088	-0.369
	0.1250	0.120	0.535	0.741	0.828	0.831	0.764	0.627	0.407	0.039
	0.2500	0.074	0.484	0.695	0.800	0.828	0.787	0.677	0.481	0.134
	0.3750	0.047	0.457	0.672	0.783	0.818	0.786	0.686	0.499	0.161
	0.5000	-0.024	0.366	0.579	0.705	0.768	0.770	0.701	0.532	0.197
	0.5625	-0.139	0.108	0.264	0.368	0.438	0.478	0.486	0.454	0.347
0.4	0.0000	0.434	0.703	0.783	0.761	0.668	0.514	0.300	0.013	-0.403
	0.1250	0.129	0.527	0.714	0.783	0.770	0.692	0.553	0.343	0.011
	0.2500	0.063	0.448	0.646	0.743	0.766	0.725	0.622	0.443	0.135
	0.3750	0.022	0.406	0.608	0.713	0.748	0.720	0.630	0.467	0.174
	0.5000	-0.068	0.293	0.493	0.617	0.687	0.703	0.655	0.508	0.212
	0.5625	-0.186	0.056	0.210	0.317	0.393	0.441	0.462	0.447	0.370
0.5	0.0000	0.464	0.690	0.741	0.701	0.597	0.441	0.234	-0.036	-0.413
	0.1250	0.136	0.519	0.689	0.740	0.714	0.629	0.491	0.292	-0.009
	0.2500	0.054	0.416	0.604	0.696	0.715	0.673	0.575	0.410	0.134
	0.3750	0.001	0.360	0.552	0.653	0.687	0.664	0.584	0.439	0.183
	0.5000	-0.102	0.232	0.422	0.544	0.618	0.644	0.611	0.482	0.219
	0.5625	-0.220	0.014	0.164	0.272	0.351	0.405	0.434	0.431	0.375
0.6	0.0000	0.481	0.671	0.700	0.646	0.537	0.383	0.185	-0.067	-0.410
	0.1250	0.140	0.511	0.664	0.701	0.665	0.576	0.440	0.252	-0.024
	0.2500	0.046	0.388	0.568	0.655	0.671	0.630	0.536	0.381	0.131
	0.3750	-0.016	0.321	0.503	0.602	0.637	0.617	0.547	0.417	0.190
	0.5000	-0.127	0.184	0.364	0.483	0.559	0.594	0.573	0.457	0.220
	0.5625	-0.243	-0.020	0.126	0.233	0.313	0.371	0.405	0.413	0.372
0.7	0.0000	0.489	0.649	0.661	0.598	0.487	0.336	0.148	-0.087	-0.401
	0.1250	0.144	0.503	0.640	0.664	0.621	0.530	0.398	0.220	-0.034
	0.2500	0.038	0.363	0.537	0.621	0.634	0.592	0.501	0.357	0.128
	0.3750	-0.030	0.286	0.461	0.558	0.594	0.577	0.516	0.398	0.195
	0.5000	-0.145	0.145	0.316	0.432	0.509	0.549	0.539	0.434	0.219
	0.5625	-0.259	-0.046	0.095	0.200	0.280	0.340	0.379	0.393	0.365
0.8	0.0000	0.491	0.626	0.624	0.556	0.445	0.299	0.120	-0.100	-0.389
	0.1250	0.146	0.495	0.617	0.630	0.582	0.490	0.362	0.194	-0.041
	0.2500	0.031	0.340	0.511	0.592	0.602	0.560	0.472	0.336	0.124
	0.3750	-0.041	0.257	0.425	0.521	0.558	0.544	0.491	0.382	0.197
	0.5000	-0.158	0.113	0.276	0.389	0.467	0.511	0.508	0.413	0.217
	0.5625	-0.268	-0.066	0.070	0.172	0.251	0.312	0.354	0.373	0.355
0.9	0.0000	0.490	0.603	0.591	0.520	0.409	0.268	0.098	-0.109	-0.376
	0.1250	0.147	0.486	0.595	0.599	0.547	0.456	0.332	0.173	-0.046
	0.2500	0.025	0.321	0.488	0.566	0.574	0.531	0.445	0.317	0.120
	0.3750	-0.050	0.231	0.393	0.489	0.527	0.515	0.469	0.368	0.198
	0.5000	-0.168	0.087	0.243	0.352	0.430	0.477	0.481	0.394	0.214
	0.5625	-0.274	-0.082	0.049	0.148	0.226	0.287	0.331	0.355	0.344
1.0	0.0000	0.485	0.580	0.561	0.487	0.378	0.242	0.080	-0.113	-0.363
	0.1250	0.147	0.477	0.567	0.571	0.516	0.426	0.307	0.155	-0.049
	0.2500	0.019	0.303	0.468	0.543	0.549	0.506	0.422	0.300	0.116
	0.3750	-0.057	0.209	0.365	0.460	0.501	0.490	0.451	0.355	0.199
	0.5000	-0.174	0.066	0.214	0.321	0.398	0.448	0.457	0.380	0.210
	0.5625	-0.277	-0.094	0.032	0.128	0.204	0.265	0.310	0.338	0.333

TABLE 3

Supervelocities over cropped delta wings for varying taper ratio ψ, convergence ratio ϵ, co-ordinate ξ and η'

$\psi = 0{\cdot}0625$

ϵ	η' \ ξ	-0.8	-0.6	-0.4	-0.2	0.0	+0.2	+0.4	+0.6	+0.8
0.2	0.0000	0.130	0.580	0.806	0.906	0.910	0.828	0.654	0.361	-0.140
	0.1250	0.102	0.558	0.796	0.915	0.946	0.897	0.764	0.522	0.080
	0.2500	0.103	0.563	0.805	0.930	0.966	0.924	0.796	0.558	0.118
	0.3750	0.108	0.569	0.813	0.939	0.977	0.937	0.811	0.574	0.135
	0.5000	0.113	0.574	0.819	0.946	0.986	0.945	0.820	0.583	0.144
	0.5625	0.115	0.577	0.822	0.949	0.988	0.948	0.823	0.587	0.148
	0.6250	0.118	0.579	0.824	0.951	0.991	0.951	0.826	0.590	0.151
	0.6875	0.120	0.581	0.826	0.954	0.993	0.954	0.829	0.593	0.154
	0.7500	0.122	0.584	0.829	0.956	0.996	0.956	0.831	0.595	0.157
	0.8750	0.125	0.589	0.834	0.961	1.001	0.962	0.837	0.600	0.163
	0.9375	0.086	0.307	0.437	0.514	0.552	0.553	0.517	0.425	0.234
0.3	0.0000	0.136	0.580	0.794	0.880	0.867	0.767	0.577	0.273	-0.227
	0.1250	0.101	0.550	0.779	0.888	0.908	0.849	0.708	0.466	0.042
	0.2500	0.095	0.549	0.785	0.904	0.934	0.887	0.759	0.527	0.109
	0.3750	0.097	0.554	0.794	0.916	0.951	0.906	0.784	0.556	0.140
	0.5000	0.102	0.561	0.802	0.926	0.963	0.922	0.800	0.574	0.159
	0.5625	0.105	0.564	0.806	0.931	0.968	0.928	0.806	0.579	0.166
	0.6250	0.108	0.568	0.810	0.935	0.973	0.933	0.811	0.585	0.172
	0.6875	0.111	0.571	0.814	0.939	0.977	0.937	0.816	0.590	0.177
	0.7500	0.115	0.575	0.818	0.943	0.981	0.942	0.821	0.595	0.183
	0.8750	0.122	0.582	0.825	0.951	0.990	0.952	0.831	0.607	0.193
	0.9375	0.073	0.303	0.438	0.522	0.566	0.578	0.553	0.478	0.311
0.4	0.0000	0.143	0.580	0.782	0.854	0.826	0.711	0.508	0.199	-0.288
	0.1250	0.102	0.545	0.765	0.863	0.871	0.801	0.653	0.412	0.007
	0.2500	0.090	0.539	0.768	0.878	0.901	0.848	0.718	0.492	0.096
	0.3750	0.088	0.541	0.775	0.891	0.921	0.875	0.752	0.533	0.143
	0.5000	0.091	0.546	0.783	0.902	0.936	0.893	0.774	0.558	0.171
	0.5625	0.093	0.549	0.787	0.908	0.942	0.901	0.782	0.567	0.181
	0.6250	0.096	0.553	0.792	0.913	0.947	0.907	0.790	0.575	0.190
	0.6875	0.100	0.557	0.796	0.918	0.953	0.913	0.797	0.583	0.198
	0.7500	0.103	0.561	0.801	0.923	0.959	0.920	0.803	0.590	0.206
	0.8750	0.111	0.568	0.809	0.933	0.970	0.933	0.818	0.606	0.222
	0.9375	0.056	0.294	0.433	0.521	0.571	0.590	0.576	0.517	0.378
0.5	0.0000	0.150	0.579	0.770	0.828	0.785	0.658	0.448	0.140	-0.329
	0.1250	0.105	0.541	0.752	0.839	0.836	0.756	0.602	0.362	-0.024
	0.2500	0.087	0.530	0.752	0.854	0.868	0.809	0.677	0.457	0.084
	0.3750	0.082	0.529	0.757	0.866	0.890	0.841	0.719	0.508	0.143
	0.5000	0.082	0.532	0.764	0.877	0.906	0.862	0.746	0.540	0.180
	0.5625	0.083	0.535	0.767	0.883	0.913	0.871	0.756	0.552	0.194
	0.6250	0.085	0.538	0.771	0.888	0.919	0.878	0.765	0.563	0.205
	0.6875	0.087	0.541	0.776	0.893	0.926	0.886	0.773	0.572	0.216
	0.7500	0.091	0.545	0.780	0.898	0.932	0.893	0.781	0.581	0.225
	0.8750	0.096	0.550	0.787	0.908	0.945	0.908	0.799	0.600	0.247
	0.9375	0.037	0.279	0.420	0.511	0.567	0.592	0.588	0.543	0.422
0.6	0.0000	0.157	0.578	0.758	0.802	0.747	0.610	0.396	0.093	-0.355
	0.1250	0.108	0.539	0.740	0.816	0.802	0.713	0.555	0.318	-0.049
	0.2500	0.087	0.524	0.737	0.830	0.837	0.772	0.638	0.424	0.072
	0.3750	0.077	0.519	0.740	0.842	0.860	0.807	0.686	0.484	0.142
	0.5000	0.074	0.519	0.745	0.853	0.877	0.831	0.717	0.522	0.187
	0.5625	0.073	0.521	0.748	0.857	0.884	0.840	0.729	0.536	0.204
	0.6250	0.074	0.522	0.751	0.862	0.890	0.848	0.739	0.548	0.217
	0.6875	0.076	0.525	0.755	0.867	0.896	0.856	0.748	0.559	0.230
	0.7500	0.078	0.528	0.759	0.872	0.903	0.863	0.757	0.569	0.241
	0.8750	0.079	0.529	0.762	0.880	0.915	0.880	0.776	0.591	0.264
	0.9375	0.018	0.260	0.402	0.496	0.556	0.587	0.590	0.556	0.453
0.7	0.0000	0.164	0.577	0.745	0.777	0.711	0.567	0.351	0.056	-0.371
	0.1250	0.113	0.536	0.728	0.794	0.769	0.674	0.513	0.281	-0.069
	0.2500	0.088	0.518	0.724	0.808	0.807	0.737	0.602	0.394	0.061
	0.3750	0.074	0.510	0.724	0.819	0.831	0.775	0.656	0.462	0.141
	0.5000	0.067	0.508	0.727	0.829	0.848	0.801	0.690	0.505	0.192
	0.5625	0.066	0.508	0.729	0.833	0.855	0.811	0.703	0.521	0.211
	0.6250	0.065	0.508	0.731	0.837	0.861	0.819	0.714	0.534	0.227
	0.6875	0.065	0.509	0.734	0.841	0.867	0.827	0.723	0.546	0.241
	0.7500	0.065	0.511	0.737	0.845	0.873	0.834	0.732	0.556	0.253
	0.8750	0.062	0.507	0.736	0.851	0.885	0.851	0.752	0.578	0.277
	0.9375	-0.002	0.239	0.382	0.478	0.541	0.576	0.585	0.560	0.474
0.8	0.0000	0.170	0.575	0.732	0.752	0.677	0.528	0.313	0.026	-0.380
	0.1250	0.117	0.534	0.717	0.772	0.739	0.637	0.476	0.248	-0.084
	0.2500	0.089	0.514	0.711	0.787	0.779	0.704	0.569	0.367	0.052
	0.3750	0.072	0.503	0.710	0.798	0.804	0.746	0.627	0.441	0.139
	0.5000	0.062	0.497	0.710	0.806	0.821	0.772	0.665	0.488	0.196
	0.5625	0.059	0.496	0.711	0.809	0.828	0.782	0.678	0.506	0.218
	0.6250	0.057	0.495	0.712	0.812	0.833	0.791	0.690	0.520	0.235
	0.6875	0.055	0.495	0.713	0.816	0.839	0.798	0.699	0.532	0.250
	0.7500	0.054	0.495	0.715	0.819	0.844	0.805	0.708	0.543	0.262
	0.8750	0.044	0.484	0.709	0.821	0.854	0.821	0.727	0.564	0.286
	0.9375	-0.024	0.217	0.361	0.458	0.523	0.562	0.576	0.558	0.484
0.9	0.0000	0.176	0.573	0.719	0.728	0.645	0.493	0.280	0.002	-0.383
	0.1250	0.122	0.532	0.705	0.751	0.710	0.604	0.442	0.221	-0.096
	0.2500	0.091	0.510	0.699	0.767	0.752	0.674	0.539	0.343	0.044
	0.3750	0.072	0.496	0.696	0.777	0.779	0.718	0.601	0.421	0.136
	0.5000	0.059	0.488	0.694	0.784	0.796	0.746	0.641	0.473	0.199
	0.5625	0.054	0.485	0.694	0.787	0.802	0.756	0.655	0.492	0.222
	0.6250	0.050	0.483	0.694	0.789	0.807	0.764	0.667	0.507	0.241
	0.6875	0.046	0.481	0.694	0.791	0.811	0.771	0.677	0.520	0.256
	0.7500	0.043	0.480	0.694	0.793	0.815	0.778	0.685	0.530	0.269
	0.8750	0.028	0.462	0.682	0.792	0.824	0.792	0.703	0.550	0.292
	0.9375	-0.045	0.195	0.340	0.438	0.505	0.547	0.565	0.553	0.489
1.0	0.0000	0.182	0.570	0.705	0.705	0.616	0.461	0.252	-0.017	-0.383
	0.1250	0.127	0.530	0.694	0.731	0.683	0.574	0.412	0.197	-0.105
	0.2500	0.094	0.506	0.687	0.748	0.727	0.646	0.512	0.321	0.037
	0.3750	0.071	0.490	0.683	0.758	0.755	0.692	0.577	0.404	0.134
	0.5000	0.056	0.480	0.679	0.764	0.772	0.721	0.619	0.459	0.201
	0.5625	0.049	0.475	0.678	0.766	0.778	0.732	0.634	0.479	0.226
	0.6250	0.044	0.472	0.677	0.767	0.782	0.740	0.646	0.495	0.246
	0.6875	0.039	0.468	0.675	0.768	0.786	0.746	0.656	0.508	0.262
	0.7500	0.034	0.465	0.674	0.769	0.789	0.752	0.664	0.518	0.275
	0.8750	0.012	0.441	0.657	0.764	0.795	0.764	0.679	0.536	0.296
	0.9375	-0.066	0.174	0.319	0.417	0.486	0.530	0.551	0.545	0.490

TABLE 3 *continued*

Supervelocities over cropped delta wings for varying taper ratio ψ, convergence ratio ϵ, co-ordinate ξ and η'

$\psi = 0{\cdot}1250$

ϵ	η'	ξ -0.8	-0.6	-0.4	-0.2	0.0	+0.2	+0.4	+0.6	+0.8
0.2	0.0000	0.130	0.580	0.806	0.906	0.910	0.828	0.654	0.361	-0.140
	0.1250	0.102	0.558	0.796	0.915	0.946	0.897	0.764	0.522	0.080
	0.2500	0.103	0.563	0.805	0.930	0.966	0.924	0.796	0.558	0.118
	0.3750	0.108	0.569	0.813	0.939	0.977	0.937	0.811	0.574	0.135
	0.5000	0.113	0.574	0.819	0.946	0.986	0.945	0.820	0.583	0.144
	0.5625	0.115	0.577	0.821	0.948	0.988	0.947	0.823	0.587	0.148
	0.6250	0.117	0.579	0.824	0.951	0.991	0.951	0.826	0.590	0.151
	0.6875	0.120	0.581	0.826	0.953	0.993	0.953	0.828	0.592	0.154
	0.7500	0.121	0.583	0.828	0.955	0.995	0.956	0.831	0.595	0.156
	0.8750	0.067	0.299	0.432	0.510	0.548	0.548	0.512	0.421	0.231
0.3	0.0000	0.136	0.580	0.794	0.880	0.867	0.767	0.577	0.273	-0.227
	0.1250	0.100	0.550	0.779	0.888	0.908	0.849	0.708	0.466	0.042
	0.2500	0.095	0.549	0.785	0.904	0.934	0.887	0.759	0.527	0.109
	0.3750	0.097	0.554	0.794	0.916	0.951	0.908	0.784	0.556	0.140
	0.5000	0.102	0.561	0.802	0.926	0.963	0.922	0.800	0.574	0.159
	0.5625	0.105	0.564	0.806	0.931	0.968	0.928	0.806	0.579	0.166
	0.6250	0.108	0.567	0.810	0.934	0.972	0.932	0.811	0.585	0.172
	0.6875	0.110	0.570	0.813	0.938	0.976	0.937	0.816	0.590	0.177
	0.7500	0.112	0.572	0.815	0.941	0.980	0.941	0.820	0.595	0.183
	0.8750	0.056	0.295	0.431	0.514	0.558	0.569	0.544	0.471	0.307
0.4	0.0000	0.143	0.580	0.782	0.853	0.825	0.710	0.508	0.199	-0.288
	0.1250	0.102	0.545	0.765	0.863	0.871	0.801	0.653	0.412	0.006
	0.2500	0.090	0.539	0.768	0.878	0.901	0.848	0.718	0.492	0.096
	0.3750	0.088	0.541	0.775	0.891	0.921	0.875	0.752	0.533	0.143
	0.5000	0.091	0.546	0.783	0.902	0.936	0.893	0.774	0.558	0.171
	0.5625	0.093	0.549	0.787	0.907	0.942	0.901	0.782	0.567	0.181
	0.6250	0.096	0.552	0.791	0.912	0.947	0.907	0.790	0.575	0.190
	0.6875	0.098	0.555	0.795	0.916	0.952	0.913	0.796	0.583	0.198
	0.7500	0.099	0.557	0.796	0.919	0.957	0.919	0.803	0.590	0.206
	0.8750	0.043	0.284	0.422	0.509	0.560	0.579	0.565	0.506	0.366
0.5	0.0000	0.150	0.579	0.770	0.828	0.785	0.658	0.448	0.140	-0.329
	0.1250	0.104	0.541	0.752	0.839	0.835	0.756	0.602	0.362	-0.024
	0.2500	0.087	0.530	0.752	0.854	0.868	0.809	0.677	0.457	0.084
	0.3750	0.081	0.529	0.757	0.866	0.890	0.841	0.719	0.508	0.143
	0.5000	0.081	0.532	0.763	0.877	0.906	0.862	0.746	0.540	0.180
	0.5625	0.082	0.534	0.767	0.882	0.913	0.871	0.756	0.552	0.194
	0.6250	0.084	0.536	0.770	0.887	0.919	0.878	0.765	0.563	0.206
	0.6875	0.085	0.539	0.774	0.892	0.925	0.885	0.773	0.572	0.216
	0.7500	0.085	0.538	0.774	0.894	0.929	0.892	0.782	0.582	0.227
	0.8750	0.027	0.268	0.409	0.499	0.555	0.580	0.575	0.529	0.410
0.6	0.0000	0.157	0.578	0.758	0.802	0.747	0.610	0.396	0.093	-0.355
	0.1250	0.108	0.539	0.740	0.816	0.802	0.713	0.555	0.318	-0.049
	0.2500	0.087	0.524	0.737	0.830	0.837	0.772	0.638	0.424	0.072
	0.3750	0.077	0.519	0.740	0.842	0.860	0.807	0.686	0.484	0.142
	0.5000	0.073	0.519	0.744	0.852	0.877	0.831	0.717	0.522	0.187
	0.5625	0.073	0.520	0.747	0.857	0.884	0.840	0.729	0.537	0.204
	0.6250	0.073	0.521	0.750	0.861	0.890	0.848	0.739	0.549	0.218
	0.6875	0.072	0.522	0.752	0.865	0.896	0.856	0.749	0.560	0.230
	0.7500	0.070	0.519	0.750	0.867	0.900	0.864	0.758	0.571	0.243
	0.8750	0.009	0.250	0.392	0.485	0.544	0.575	0.577	0.542	0.440
0.7	0.0000	0.164	0.577	0.745	0.777	0.711	0.567	0.351	0.056	-0.371
	0.1250	0.113	0.536	0.728	0.793	0.769	0.674	0.513	0.281	-0.069
	0.2500	0.087	0.518	0.724	0.808	0.807	0.737	0.602	0.394	0.061
	0.3750	0.074	0.510	0.724	0.819	0.831	0.775	0.656	0.462	0.141
	0.5000	0.067	0.507	0.726	0.828	0.848	0.801	0.690	0.505	0.193
	0.5625	0.064	0.507	0.728	0.832	0.855	0.811	0.703	0.521	0.212
	0.6250	0.063	0.506	0.730	0.836	0.861	0.819	0.714	0.535	0.228
	0.6875	0.061	0.505	0.730	0.839	0.867	0.827	0.724	0.547	0.242
	0.7500	0.056	0.499	0.726	0.839	0.871	0.835	0.735	0.559	0.255
	0.8750	-0.010	0.231	0.374	0.469	0.531	0.566	0.574	0.548	0.460
0.8	0.0000	0.170	0.575	0.732	0.752	0.677	0.528	0.313	0.026	-0.379
	0.1250	0.117	0.534	0.717	0.772	0.739	0.637	0.476	0.248	-0.084
	0.2500	0.089	0.514	0.711	0.787	0.779	0.704	0.569	0.367	0.052
	0.3750	0.072	0.503	0.709	0.798	0.804	0.746	0.627	0.441	0.139
	0.5000	0.061	0.497	0.710	0.805	0.821	0.773	0.665	0.489	0.196
	0.5625	0.058	0.495	0.710	0.809	0.828	0.783	0.679	0.506	0.218
	0.6250	0.054	0.492	0.710	0.812	0.833	0.791	0.690	0.521	0.235
	0.6875	0.050	0.489	0.709	0.814	0.839	0.799	0.701	0.533	0.251
	0.7500	0.043	0.481	0.703	0.813	0.843	0.808	0.711	0.546	0.265
	0.8750	-0.028	0.212	0.355	0.451	0.516	0.554	0.567	0.548	0.473
0.9	0.0000	0.176	0.572	0.719	0.728	0.645	0.493	0.280	0.002	-0.383
	0.1250	0.122	0.532	0.705	0.751	0.710	0.604	0.442	0.221	-0.096
	0.2500	0.091	0.509	0.699	0.767	0.752	0.674	0.539	0.343	0.044
	0.3750	0.071	0.496	0.696	0.777	0.779	0.718	0.601	0.421	0.136
	0.5000	0.057	0.487	0.694	0.784	0.796	0.746	0.641	0.473	0.199
	0.5625	0.052	0.484	0.693	0.787	0.802	0.756	0.656	0.492	0.222
	0.6250	0.046	0.480	0.692	0.789	0.807	0.765	0.668	0.508	0.242
	0.6875	0.040	0.474	0.689	0.790	0.812	0.773	0.678	0.521	0.258
	0.7500	0.031	0.462	0.680	0.787	0.816	0.781	0.689	0.534	0.272
	0.8750	-0.046	0.194	0.337	0.434	0.500	0.541	0.558	0.545	0.480
1.0	0.0000	0.182	0.570	0.705	0.705	0.616	0.461	0.252	-0.017	-0.383
	0.1250	0.127	0.530	0.694	0.730	0.683	0.574	0.412	0.197	-0.105
	0.2500	0.093	0.506	0.687	0.748	0.727	0.646	0.512	0.321	0.037
	0.3750	0.071	0.490	0.683	0.758	0.755	0.692	0.577	0.404	0.134
	0.5000	0.054	0.478	0.679	0.764	0.772	0.722	0.619	0.459	0.201
	0.5625	0.047	0.473	0.677	0.766	0.778	0.732	0.635	0.479	0.226
	0.6250	0.040	0.468	0.675	0.767	0.783	0.741	0.647	0.495	0.246
	0.6875	0.032	0.460	0.671	0.767	0.787	0.748	0.658	0.509	0.263
	0.7500	0.020	0.445	0.659	0.763	0.791	0.757	0.668	0.522	0.278
	0.8750	-0.063	0.177	0.320	0.417	0.485	0.528	0.548	0.540	0.484

TABLE 3 *continued*

Supervelocities over cropped delta wings for varying taper ratio ψ, convergence ratio ϵ, co-ordinate ξ and η'

$\psi = 0{\cdot}3125$

ϵ	η'	ξ -0.8	-0.6	-0.4	-0.2	0.0	+0.2	+0.4	+0.6	+0.8
0.2	0.0000	0.129	0.580	0.805	0.905	0.910	0.828	0.653	0.361	-0.140
	0.1250	0.102	0.558	0.796	0.915	0.946	0.897	0.764	0.522	0.080
	0.2500	0.103	0.562	0.804	0.929	0.966	0.923	0.796	0.558	0.118
	0.3750	0.107	0.568	0.812	0.938	0.976	0.936	0.810	0.573	0.134
	0.5000	0.109	0.570	0.814	0.942	0.982	0.942	0.817	0.581	0.143
	0.5625	0.106	0.566	0.810	0.938	0.979	0.940	0.817	0.583	0.146
	0.6250	0.094	0.546	0.783	0.909	0.952	0.921	0.807	0.582	0.152
	0.6875	0.055	0.292	0.424	0.501	0.538	0.540	0.502	0.412	0.225
0.3	0.0000	0.136	0.579	0.793	0.879	0.867	0.767	0.576	0.272	-0.227
	0.1250	0.100	0.549	0.779	0.888	0.907	0.848	0.708	0.466	0.042
	0.2500	0.093	0.548	0.784	0.903	0.933	0.887	0.758	0.527	0.109
	0.3750	0.095	0.552	0.791	0.914	0.949	0.907	0.783	0.555	0.140
	0.5000	0.094	0.552	0.793	0.918	0.956	0.917	0.797	0.573	0.159
	0.5625	0.090	0.544	0.784	0.910	0.951	0.917	0.801	0.579	0.168
	0.6250	0.079	0.515	0.742	0.864	0.912	0.891	0.794	0.590	0.188
	0.6875	0.043	0.281	0.417	0.499	0.543	0.554	0.528	0.454	0.291
0.4	0.0000	0.142	0.578	0.781	0.853	0.825	0.710	0.508	0.199	-0.288
	0.1250	0.100	0.544	0.764	0.862	0.870	0.800	0.653	0.412	0.007
	0.2500	0.088	0.536	0.766	0.876	0.900	0.847	0.717	0.492	0.097
	0.3750	0.084	0.536	0.770	0.887	0.918	0.874	0.752	0.533	0.143
	0.5000	0.080	0.532	0.768	0.889	0.927	0.889	0.773	0.559	0.174
	0.5625	0.073	0.520	0.753	0.876	0.919	0.889	0.781	0.572	0.189
	0.6250	0.065	0.485	0.701	0.819	0.871	0.861	0.781	0.595	0.221
	0.6875	0.028	0.267	0.405	0.491	0.540	0.558	0.543	0.483	0.342
0.5	0.0000	0.148	0.577	0.769	0.826	0.785	0.658	0.448	0.141	-0.329
	0.1250	0.102	0.539	0.750	0.838	0.835	0.755	0.602	0.362	-0.024
	0.2500	0.084	0.527	0.749	0.851	0.867	0.808	0.677	0.457	0.084
	0.3750	0.075	0.522	0.750	0.861	0.887	0.840	0.719	0.509	0.145
	0.5000	0.066	0.512	0.742	0.860	0.896	0.859	0.748	0.545	0.185
	0.5625	0.059	0.496	0.722	0.842	0.887	0.862	0.760	0.563	0.206
	0.6250	0.052	0.456	0.662	0.778	0.832	0.832	0.765	0.598	0.247
	0.6875	0.012	0.252	0.391	0.479	0.533	0.557	0.549	0.502	0.380
0.6	0.0000	0.154	0.576	0.756	0.801	0.747	0.610	0.396	0.094	-0.355
	0.1250	0.105	0.536	0.738	0.814	0.801	0.713	0.555	0.319	-0.049
	0.2500	0.082	0.519	0.733	0.828	0.836	0.772	0.639	0.425	0.073
	0.3750	0.068	0.509	0.731	0.836	0.857	0.807	0.688	0.486	0.144
	0.5000	0.055	0.493	0.717	0.831	0.866	0.831	0.723	0.529	0.194
	0.5625	0.047	0.473	0.692	0.809	0.855	0.835	0.740	0.553	0.219
	0.6250	0.040	0.429	0.627	0.740	0.797	0.803	0.749	0.596	0.267
	0.6875	-0.003	0.236	0.376	0.466	0.523	0.551	0.550	0.512	0.407
0.7	0.0000	0.160	0.573	0.743	0.775	0.711	0.567	0.352	0.056	-0.370
	0.1250	0.109	0.532	0.725	0.792	0.769	0.674	0.514	0.281	-0.068
	0.2500	0.082	0.512	0.719	0.805	0.806	0.737	0.603	0.395	0.063
	0.3750	0.063	0.497	0.713	0.813	0.829	0.777	0.658	0.464	0.143
	0.5000	0.046	0.475	0.693	0.804	0.839	0.804	0.698	0.514	0.200
	0.5625	0.036	0.452	0.664	0.779	0.826	0.809	0.720	0.541	0.228
	0.6250	0.029	0.404	0.596	0.707	0.765	0.777	0.732	0.593	0.281
	0.6875	-0.017	0.221	0.361	0.453	0.511	0.543	0.547	0.518	0.426
0.8	0.0000	0.165	0.571	0.729	0.751	0.677	0.529	0.314	0.027	-0.379
	0.1250	0.112	0.529	0.713	0.770	0.739	0.638	0.477	0.249	-0.083
	0.2500	0.082	0.506	0.705	0.784	0.778	0.705	0.571	0.368	0.054
	0.3750	0.060	0.487	0.696	0.791	0.803	0.748	0.631	0.444	0.142
	0.5000	0.039	0.459	0.671	0.779	0.813	0.778	0.676	0.499	0.204
	0.5625	0.027	0.433	0.638	0.750	0.798	0.785	0.701	0.529	0.235
	0.6250	0.019	0.382	0.568	0.677	0.736	0.752	0.715	0.587	0.291
	0.6875	-0.030	0.207	0.347	0.439	0.500	0.534	0.543	0.519	0.439
0.9	0.0000	0.170	0.568	0.716	0.727	0.646	0.494	0.281	0.003	-0.382
	0.1250	0.116	0.526	0.701	0.749	0.711	0.605	0.443	0.222	-0.095
	0.2500	0.082	0.500	0.692	0.764	0.752	0.675	0.541	0.345	0.046
	0.3750	0.057	0.477	0.681	0.770	0.779	0.722	0.605	0.425	0.139
	0.5000	0.032	0.444	0.651	0.756	0.789	0.755	0.654	0.484	0.207
	0.5625	0.020	0.415	0.615	0.725	0.773	0.763	0.683	0.518	0.240
	0.6250	0.010	0.362	0.543	0.650	0.710	0.729	0.699	0.581	0.298
	0.6875	-0.041	0.195	0.334	0.427	0.488	0.525	0.536	0.518	0.448
1.0	0.0000	0.175	0.564	0.703	0.705	0.617	0.463	0.253	-0.016	-0.382
	0.1250	0.119	0.522	0.689	0.729	0.684	0.575	0.414	0.198	-0.104
	0.2500	0.083	0.494	0.680	0.745	0.728	0.648	0.514	0.323	0.039
	0.3750	0.055	0.468	0.666	0.751	0.756	0.697	0.582	0.408	0.137
	0.5000	0.027	0.431	0.632	0.734	0.767	0.734	0.634	0.471	0.209
	0.5625	0.014	0.399	0.594	0.701	0.750	0.743	0.666	0.506	0.244
	0.6250	0.002	0.345	0.521	0.627	0.687	0.708	0.684	0.574	0.302
	0.6875	-0.052	0.183	0.322	0.415	0.477	0.515	0.529	0.516	0.453

TABLE 3 *continued*

Supervelocities over cropped delta wings for varying taper ratio ψ, convergence ratio ϵ, co-ordinate ξ and η'

$\psi = 0{\cdot}4375$

ϵ	η' \ ξ	-0.8	-0.6	-0.4	-0.2	0.0	+0.2	+0.4	+0.6	+0.8
0.2	0.0000	0.128	0.579	0.804	0.904	0.909	0.827	0.653	0.360	-0.141
	0.1250	0.101	0.557	0.794	0.914	0.944	0.896	0.763	0.521	0.079
	0.2500	0.100	0.560	0.802	0.927	0.963	0.921	0.794	0.557	0.117
	0.3750	0.100	0.560	0.803	0.930	0.969	0.930	0.806	0.571	0.133
	0.5000	0.083	0.524	0.753	0.874	0.919	0.893	0.789	0.573	0.151
	0.5625	0.051	0.287	0.419	0.496	0.533	0.534	0.496	0.406	0.218
0.3	0.0000	0.134	0.577	0.791	0.877	0.865	0.766	0.576	0.272	-0.227
	0.1250	0.097	0.547	0.776	0.885	0.905	0.847	0.707	0.465	0.042
	0.2500	0.089	0.543	0.779	0.898	0.929	0.884	0.757	0.526	0.109
	0.3750	0.083	0.537	0.775	0.898	0.936	0.899	0.779	0.555	0.142
	0.5000	0.070	0.488	0.702	0.818	0.866	0.853	0.770	0.582	0.190
	0.5625	0.036	0.274	0.409	0.491	0.534	0.544	0.517	0.443	0.279
0.4	0.0000	0.139	0.575	0.778	0.850	0.823	0.709	0.507	0.200	-0.287
	0.1250	0.096	0.539	0.759	0.858	0.867	0.799	0.652	0.411	0.007
	0.2500	0.080	0.528	0.757	0.869	0.894	0.844	0.717	0.492	0.098
	0.3750	0.069	0.514	0.745	0.863	0.901	0.865	0.751	0.537	0.149
	0.5000	0.058	0.455	0.657	0.768	0.819	0.816	0.751	0.586	0.223
	0.5625	0.021	0.259	0.396	0.480	0.529	0.545	0.528	0.467	0.325
0.5	0.0000	0.143	0.571	0.764	0.823	0.783	0.657	0.448	0.142	-0.327
	0.1250	0.096	0.532	0.744	0.832	0.831	0.754	0.602	0.363	-0.023
	0.2500	0.074	0.514	0.736	0.841	0.861	0.806	0.677	0.459	0.087
	0.3750	0.058	0.493	0.716	0.830	0.867	0.833	0.723	0.517	0.153
	0.5000	0.047	0.426	0.617	0.726	0.779	0.783	0.731	0.587	0.247
	0.5625	0.007	0.245	0.382	0.468	0.520	0.541	0.531	0.482	0.358
0.6	0.0000	0.147	0.567	0.749	0.796	0.745	0.611	0.398	0.095	-0.353
	0.1250	0.097	0.526	0.729	0.808	0.798	0.712	0.557	0.321	-0.047
	0.2500	0.071	0.502	0.716	0.815	0.829	0.771	0.641	0.428	0.077
	0.3750	0.050	0.474	0.689	0.799	0.834	0.802	0.695	0.498	0.155
	0.5000	0.038	0.400	0.584	0.689	0.743	0.753	0.711	0.584	0.265
	0.5625	-0.006	0.231	0.368	0.456	0.509	0.534	0.530	0.489	0.381
0.7	0.0000	0.151	0.563	0.734	0.771	0.710	0.569	0.354	0.059	-0.368
	0.1250	0.099	0.520	0.714	0.784	0.766	0.675	0.516	0.284	-0.066
	0.2500	0.068	0.492	0.698	0.790	0.800	0.738	0.607	0.400	0.067
	0.3750	0.044	0.457	0.664	0.770	0.805	0.774	0.670	0.479	0.156
	0.5000	0.030	0.378	0.555	0.658	0.712	0.726	0.692	0.578	0.277
	0.5625	-0.017	0.218	0.355	0.443	0.498	0.526	0.526	0.492	0.396
0.8	0.0000	0.155	0.558	0.719	0.746	0.677	0.531	0.317	0.029	-0.376
	0.1250	0.100	0.513	0.699	0.762	0.737	0.640	0.480	0.253	-0.080
	0.2500	0.066	0.482	0.680	0.767	0.773	0.708	0.577	0.374	0.058
	0.3750	0.040	0.442	0.641	0.743	0.778	0.749	0.647	0.461	0.154
	0.5000	0.023	0.358	0.530	0.630	0.685	0.701	0.673	0.571	0.285
	0.5625	-0.027	0.207	0.343	0.432	0.488	0.517	0.521	0.492	0.406
0.9	0.0000	0.158	0.552	0.704	0.723	0.647	0.497	0.285	0.006	-0.379
	0.1250	0.102	0.507	0.685	0.741	0.710	0.609	0.448	0.226	-0.092
	0.2500	0.066	0.472	0.664	0.746	0.748	0.680	0.549	0.351	0.051
	0.3750	0.037	0.429	0.621	0.719	0.753	0.725	0.625	0.444	0.153
	0.5000	0.016	0.341	0.508	0.606	0.661	0.679	0.656	0.563	0.289
	0.5625	-0.036	0.197	0.333	0.421	0.477	0.508	0.514	0.489	0.412
1.0	0.0000	0.161	0.546	0.689	0.701	0.619	0.467	0.257	-0.013	-0.379
	0.1250	0.104	0.501	0.671	0.721	0.685	0.580	0.419	0.203	-0.101
	0.2500	0.066	0.463	0.648	0.725	0.725	0.655	0.523	0.331	0.044
	0.3750	0.034	0.416	0.602	0.697	0.730	0.703	0.605	0.427	0.150
	0.5000	0.011	0.326	0.489	0.585	0.639	0.658	0.639	0.554	0.291
	0.5625	-0.043	0.188	0.323	0.411	0.467	0.499	0.506	0.486	0.415

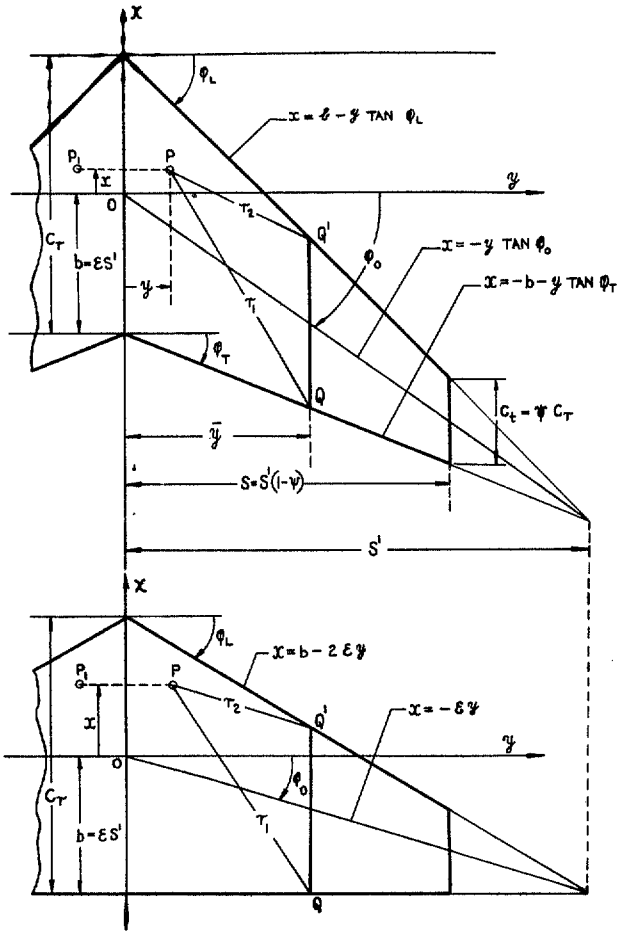

FIG. 1. Cropped tapered arrowhead and delta wing plan-forms.

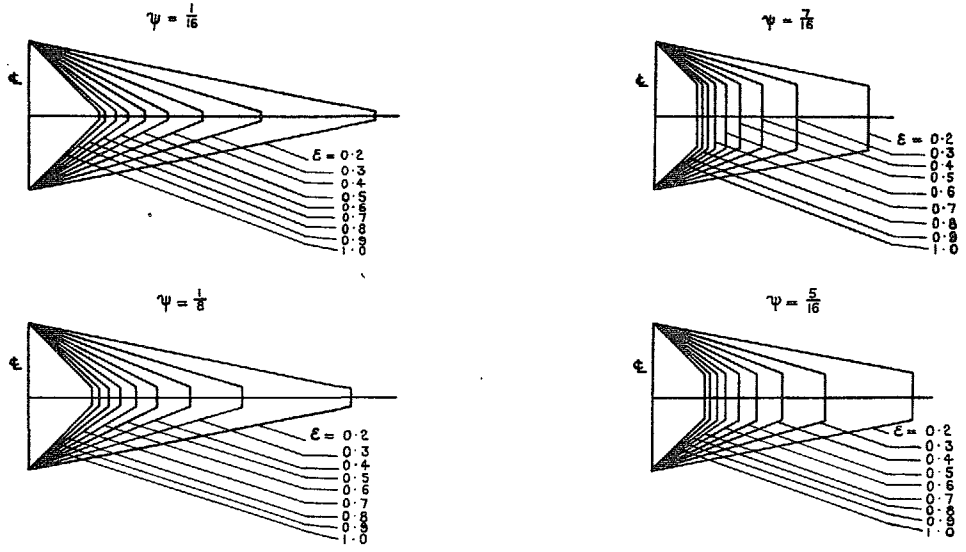

FIG. 2. Four families of affine cropped rhombus wing plan-forms.

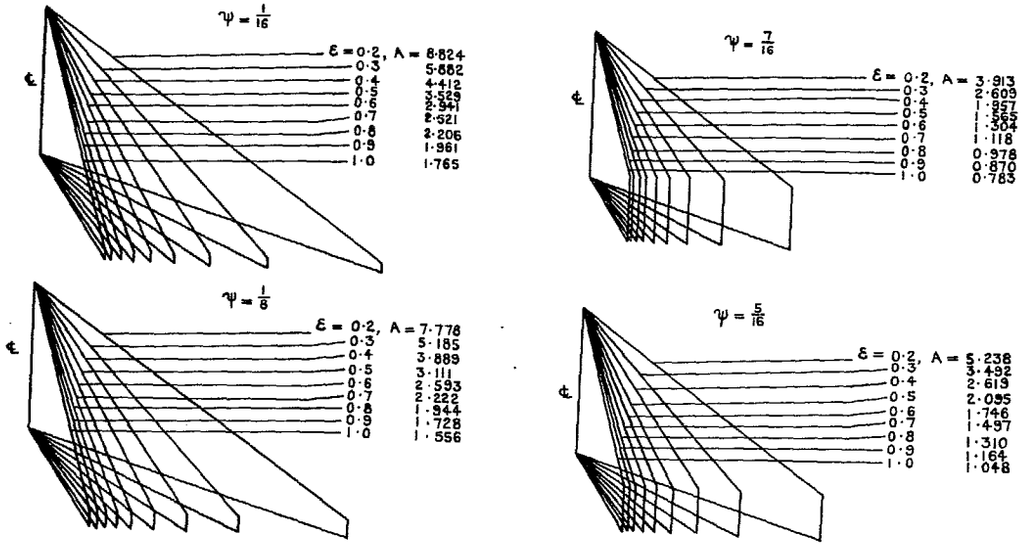

FIG. 3. Four families of affine cropped arrowhead wing plan-forms ($K = 2{\cdot}5$).

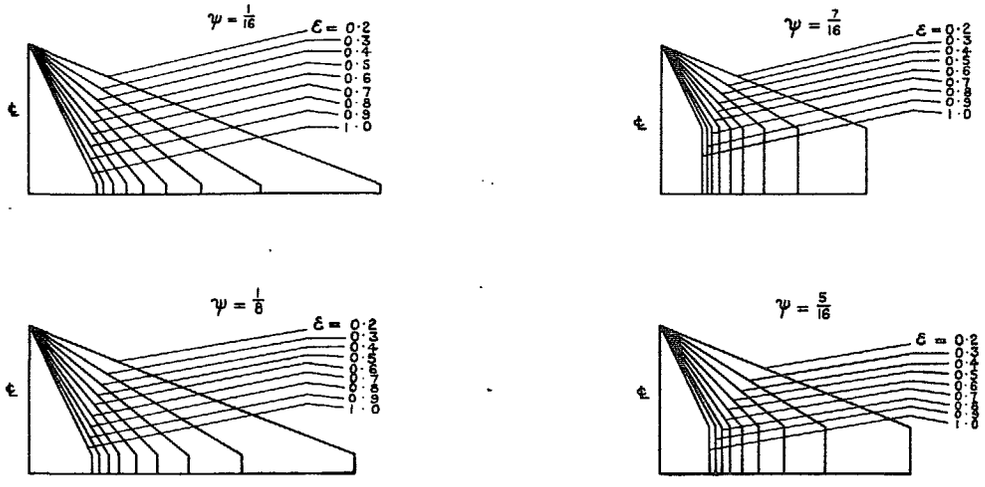

FIG 4. Four families of affine cropped delta wing plan-forms.

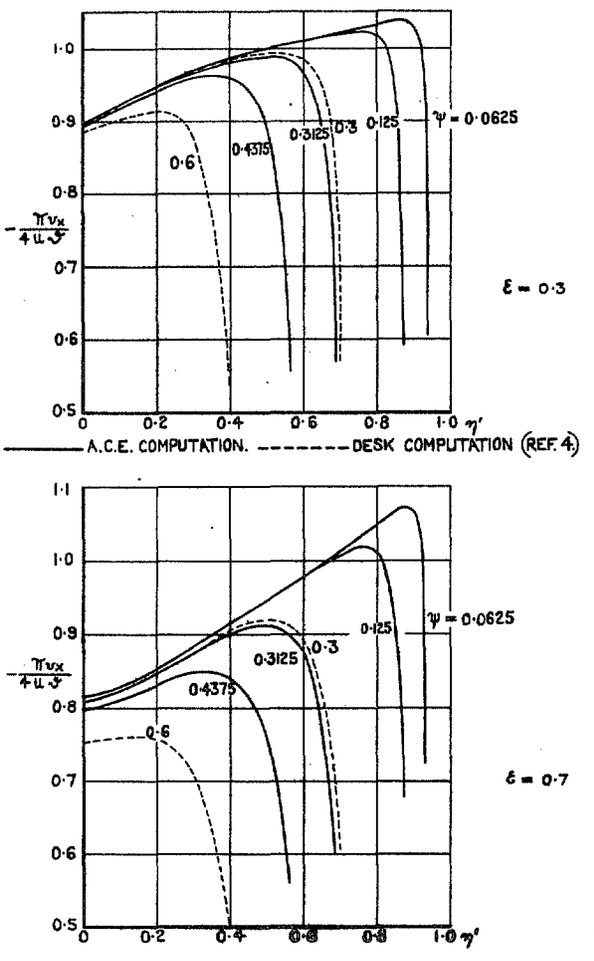

FIG. 5. Supervelocities along mid-chord lines of two groups of cropped rhombus wings obtained by two alternative computational methods ($\varepsilon = 0{\cdot}3$ and $0{\cdot}7$).

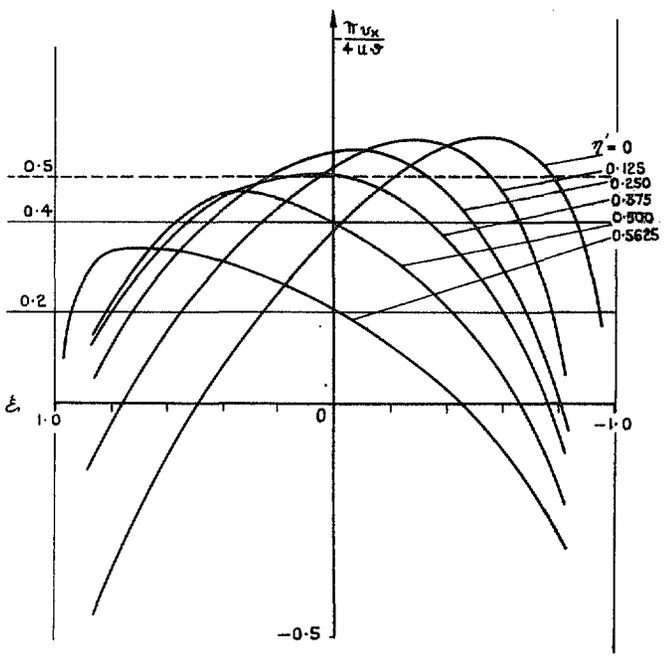

FIG. 6. Illustrative example of velocity distribution over a cropped arrowhead wing ($K = 2{\cdot}5$. $\varepsilon = 1{\cdot}0$. $\psi = 0{\cdot}4375$. $\varphi_0 = 68° 12'$. $A = 0{\cdot}783$).

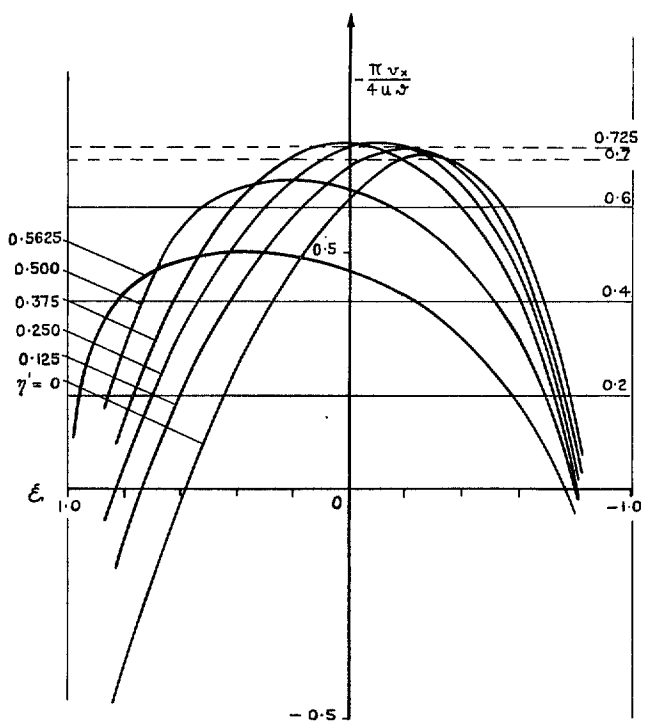

FIG. 7. Illustrative example of velocity distribution over a cropped delta wing ($\varepsilon = 1{\cdot}0$. $\psi = 0{\cdot}4375$. $\varphi_0 = 45°$. $A = 0{\cdot}783$).

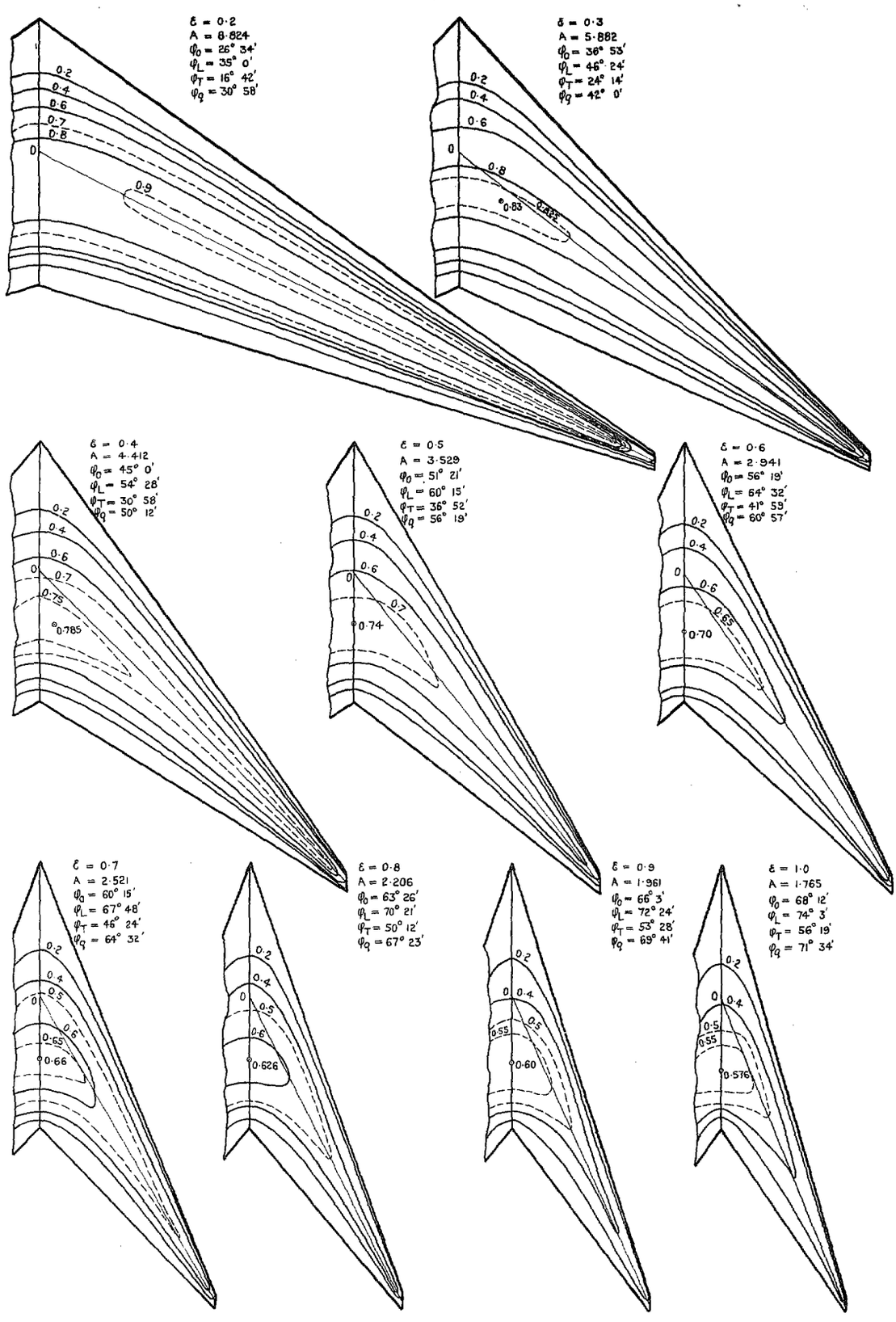

FIG. 8. Isobar patterns on a family of affine arrowhead wings of small taper ratio ($\psi = 0{\cdot}0625$. $K = 2{\cdot}5$. Varying ε, φ_0 and A).

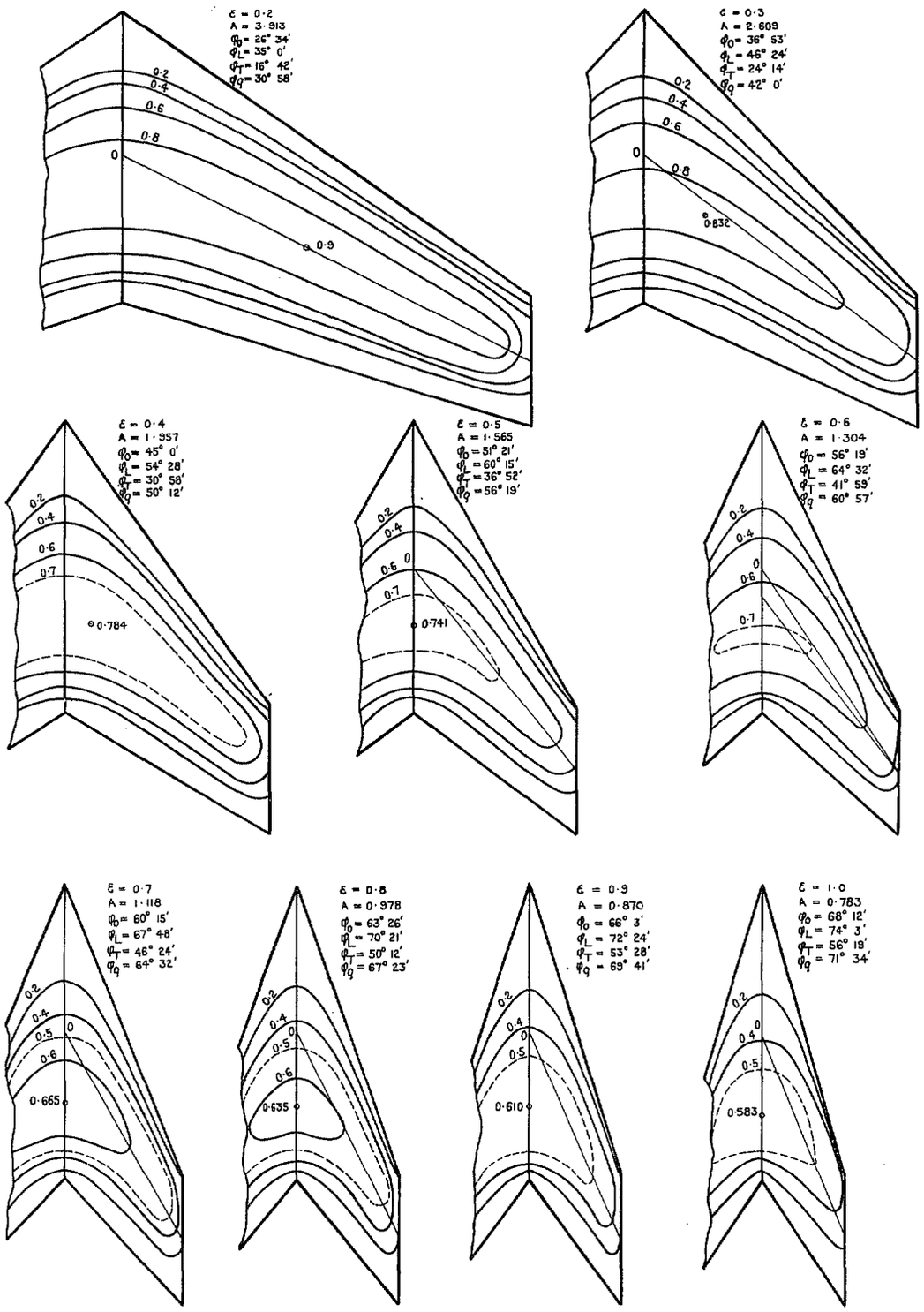

FIG. 9. Isobar patterns on a family of affine arrowhead wings of large taper ratio ($\psi = 0{\cdot}4375$. $K = 2{\cdot}5$. Varying ε, φ_0 and A).

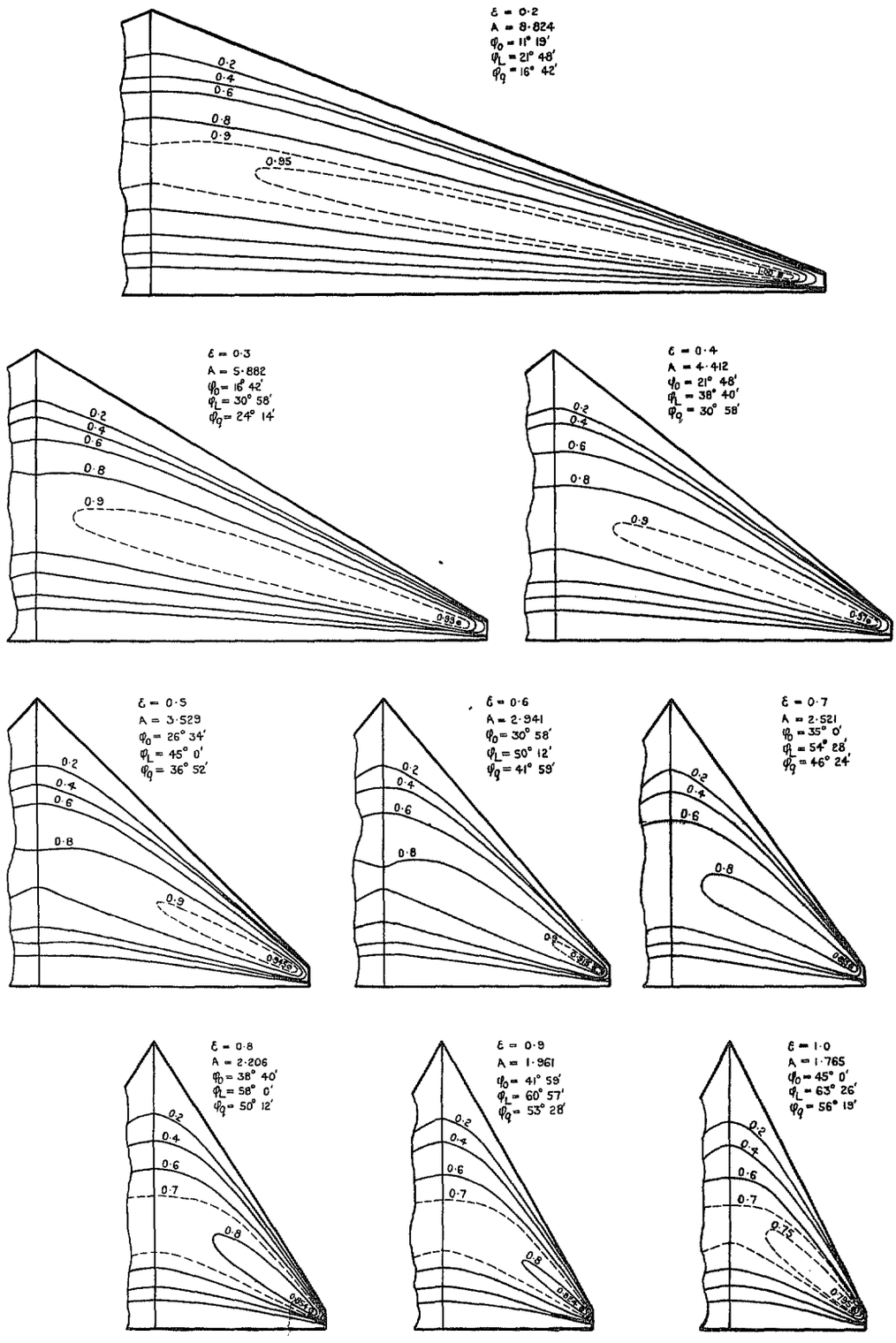

FIG .10. Isobar patterns on a family of affine cropped delta wings of small taper ratio ($\psi = 0{\cdot}0625$. Varying ε, φ_0 and A).

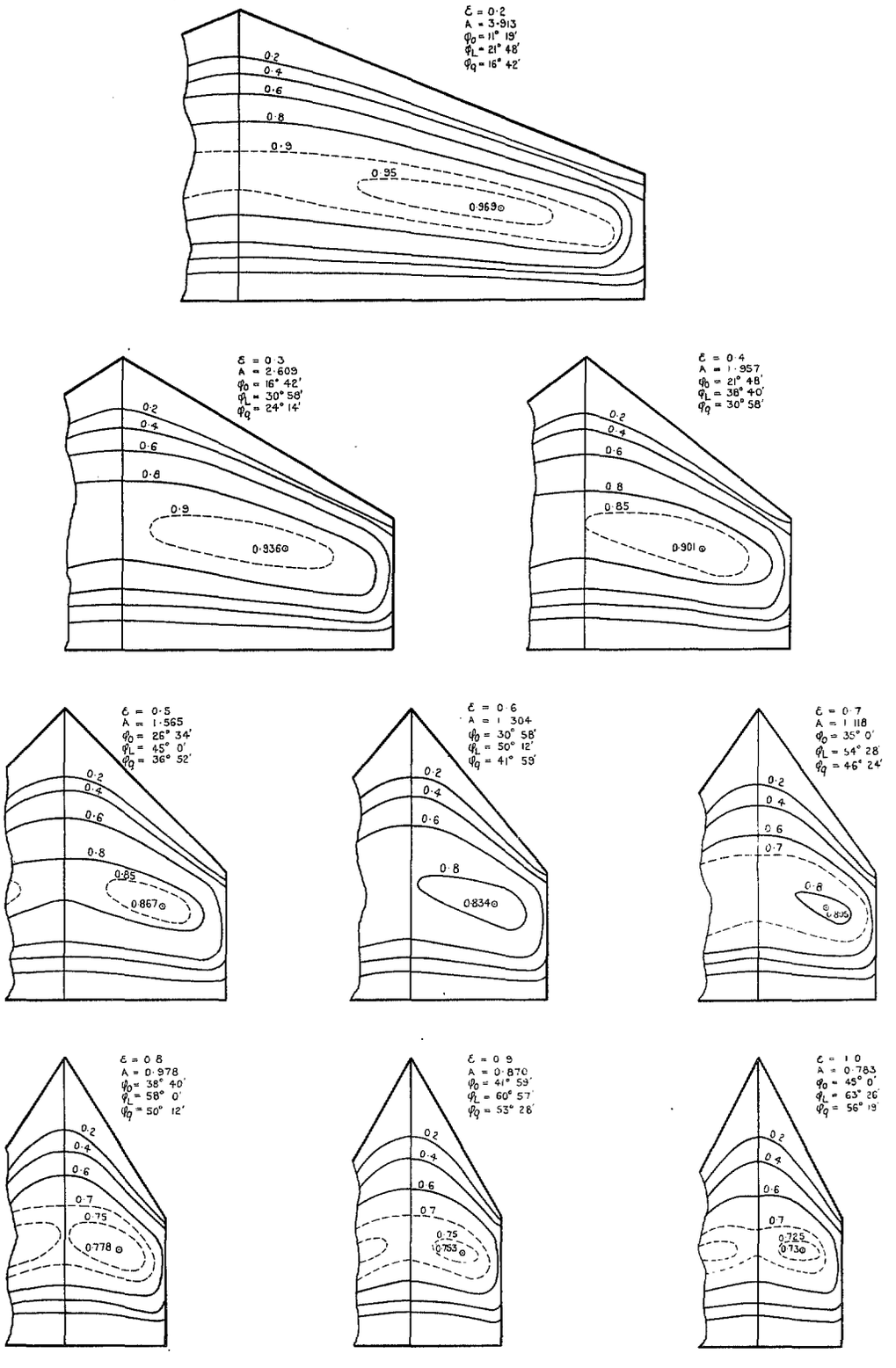

FIG. 11. Isobar patterns on a family of affine cropped delta wings of large taper ratio ($\psi = 0{\cdot}4375$. Varying ε, φ_0 and A).

Publications of the Aeronautical Research Council

ANNUAL TECHNICAL REPORTS OF THE AERONAUTICAL RESEARCH COUNCIL (BOUND VOLUMES)

1939 Vol. I. Aerodynamics General, Performance, Airscrews, Engines. 50*s.* (52*s.*).
Vol. II. Stability and Control, Flutter and Vibration, Instruments, Structures, Seaplanes, etc. 63*s.* (65*s.*)

1940 Aero and Hydrodynamics, Aerofoils, Airscrews, Engines, Flutter, Icing, Stability and Control, Structures, and a miscellaneous section. 50*s.* (52*s.*)

1941 Aero and Hydrodynamics, Aerofoils, Airscrews, Engines, Flutter, Stability and Control, Structures. 63*s.* (65*s.*)

1942 Vol. I. Aero and Hydrodynamics, Aerofoils, Airscrews, Engines. 75*s.* (77*s.*)
Vol. II. Noise, Parachutes, Stability and Control, Structures, Vibration, Wind Tunnels. 47*s.* 6*d.* (49*s.* 6*d.*)

1943 Vol. I. Aerodynamics, Aerofoils, Airscrews. 80*s.* (82*s.*)
Vol. II. Engines, Flutter, Materials, Parachutes, Performance, Stability and Control, Structures. 90*s.* (92*s.* 9*d.*)

1944 Vol. I. Aero and Hydrodynamics, Aerofoils, Aircraft, Airscrews, Controls. 84*s.* (86*s.* 6*d.*)
Vol. II. Flutter and Vibration, Materials, Miscellaneous, Navigation, Parachutes, Performance, Plates and Panels, Stability, Structures, Test Equipment, Wind Tunnels. 84*s.* (86*s.* 6*d.*)

1945 Vol. I. Aero and Hydrodynamics, Aerofoils. 130*s.* (132*s.* 9*d.*)
Vol. II. Aircraft, Airscrews, Controls. 130*s.* (132*s.* 9*d.*)
Vol. III. Flutter and Vibration, Instruments, Miscellaneous, Parachutes, Plates and Panels, Propulsion. 130*s.* (132*s.* 6*d.*)
Vol. IV. Stability, Structures, Wind Tunnels, Wind Tunnel Technique. 130*s.* (132*s.* 6*d.*)

Annual Reports of the Aeronautical Research Council—

1937 2*s.* (2*s.* 2*d.*) 1938 1*s.* 6*d.* (1*s.* 8*d.*) 1939–48 3*s.* (3*s.* 5*d.*)

Index to all Reports and Memoranda published in the Annual Technical Reports, and separately—

April, 1950 - - - - R. & M. 2600 2*s.* 6*d.* (2*s.* 10*d.*)

Author Index to all Reports and Memoranda of the Aeronautical Research Council—

1909—January, 1954 R. & M. No. 2570 15*s.* (15*s.* 8*d.*)

Indexes to the Technical Reports of the Aeronautical Research Council—

December 1, 1936—June 30, 1939	R. & M. No. 1850	1*s.* 3*d.* (1*s.* 5*d.*)
July 1, 1939—June 30, 1945	R. & M. No. 1950	1*s.* (1*s.* 2*d.*)
July 1, 1945—June 30, 1946	R. & M. No. 2050	1*s.* (1*s.* 2*d.*)
July 1, 1946—December 31, 1946	R. & M. No. 2150	1*s.* 3*d.* (1*s.* 5*d.*)
January 1, 1947—June 30, 1947	R. & M. No. 2250	1*s.* 3*d.* (1*s.* 5*d.*)

Published Reports and Memoranda of the Aeronautical Research Council—

Between Nos. 2251–2349	R. & M. No. 2350	1*s.* 9*d.* (1*s.* 11*d.*)
Between Nos. 2351–2449	R. & M. No. 2450	2*s.* (2*s.* 2*d.*)
Between Nos. 2451–2549	R. & M. No. 2550	2*s.* 6*d.* (2*s.* 10*d.*)
Between Nos. 2551–2649	R. & M. No. 2650	2*s.* 6*d.* (2*s.* 10*d.*)
Between Nos. 2651–2749	R. & M. No. 2750	2*s.* 6*d.* (2*s.* 10*d.*)

Prices in brackets include postage

HER MAJESTY'S STATIONERY OFFICE

York House, Kingsway, London W.C.2; 423 Oxford Street, London W.1; 13a Castle Street, Edinburgh 2; 39 King Street, Manchester 2; 2 Edmund Street, Birmingham 3; 109 St. Mary Street, Cardiff; Tower Lane, Bristol 1; 80 Chichester Street, Belfast, *or through any bookseller.*

S.O. Code No. 23-3008